Quaternary Science Reviews 245 (2020) 106520

Contents lists available at ScienceDirect

Quaternary Science Reviews

journal homepage: www.elsevier.com/locate/quascirev

A new perspective of the Alboran Upwelling System reconstruction during the Marine Isotope Stage 11: A high-resolution coccolithophore record

Alba González-Lanchas [a, *], José-Abel Flores [a], Francisco J. Sierro [a], María Ángeles Bárcena [a], Andrés S. Rigual-Hernández [a], Dulce Oliveira [b, c], Lucía A. Azibeiro [a], Maria Marino [d], Patrizia Maiorano [d], Aleix Cortina [e], Isabel Cacho [f], Joan O. Grimalt [e]

[a] Departamento de Geología, Universidad de Salamanca, 37008, Salamanca, Spain
[b] Centro de Ciências do Mar (CCMAR), Universidade do Algarve, Campus de Gambelas, 8005-139, Faro, Portugal
[c] Divisão de Geologia e Georecursos Marinhos, Instituto Português do Mar e da Atmosfera (IPMA), Av. Doutor Alfredo Magalhães Ramalho 6, 1495-165, Algés, Portugal
[d] Dipartimento di Scienze della Terra e Geoambientali, Università degli Studi di Bari Aldo Moro, Bari, Italy
[e] Department of Environmental Chemistry, IDAEA-CSIC, Barcelona, 08034, Spain
[f] GRC Geociències Marines, Departament de Dinàmica de la Terra i de l'Oceà, Facultat de Ciències de la Terra, Universitat de Barcelona, Barcelona, 08028, Spain

ARTICLE INFO

Article history:
Received 5 March 2020
Received in revised form
23 July 2020
Accepted 23 July 2020
Available online 3 September 2020

Keywords:
Palaeoceanography
Interglacial
Marine isotope stage 11
Alboran sea
Western europe
Micropaleontology
Coccolithophore primary productivity
North atlantic oscillation

ABSTRACT

A high-resolution study of the MIS 12/MIS 11 transition and the MIS 11 (430–376 kyr) coccolithophore assemblages at Ocean Drilling Program Site 977 was conducted to reconstruct the palaeoceanographic and climatic changes in the Alboran Sea from the variability in surface water conditions. The nannofossil record was integrated with the planktonic oxygen and carbon stable isotopes, as well as the $U^{k'}_{37}$ Sea Surface Temperature (SST) at the studied site during the investigated interval. The coccolithophore primary productivity, reconstructed from the PPP (primary productivity proxy = absolute values of *Gephyrocapsa caribbeanica* + small *Gephyrocapsa* group) revealed pronounced fluctuations, that were strongly associated with variations in the intensity of the regional *Alboran Upwelling System*. The comparison of the nannoplankton record with opal phytolith content for the studied site and the already available pollen record at the nearby Integrated Ocean Drilling Program Site U1385, suggests an association of the upwelling dynamics with the variability of the North Atlantic Oscillation-*like* (NAO-*like*) phase. High PPP during positive (+) NAO-*like* phases is the result of intensified upwelling, owing to the complete development of the surface hydrological structures at the Alboran Sea. This scenario was identified during the MIS 12/MIS 11 transition (428-422 kyr), the late MIS 11c (405-397 kyr), and MIS11 b to MIS 11a (397-376 kyr). Two short-term minima in the PPP and SST were observed during MIS 11 b and were coeval with the North Atlantic Heinrich-*type* (Ht) events Ht3 (~390 kyr) and Ht2 (~384 kyr). Increased abundance of the subpolar *Coccolithus pelagicus* subsp. *pelagicus* and *Gephyrocapsa muellerae* was consistent with the inflow of cold surface waters into the Mediterranean Sea during the Ht events. Lowered PPP during negative (−) NAO-*like* phases is the result of moderate upwelling by the incomplete development of surface hydrological structures at the Alboran Sea. This scenario is expressed during the early MIS 11c (422-405 kyr). Overall, the results of our study provide evidence of the important role of atmospheric circulation patterns in the North Atlantic region for controlling phytoplankton primary production and oceanographic circulation dynamics in the Western Mediterranean during MIS 11.

1. Introduction

The Mid-Brunhes interval, spanning from Pleistocene Marine

* Corresponding author.
E-mail address: lanchas@usal.es (A. González-Lanchas).

https://doi.org/10.1016/j.quascirev.2020.106520
0277-3791/

Isotope Stages (MIS) 14 to 9 (Barker et al., 2006; Jansen et al., 1986), is a critical period for global climate change. Following the Mid-Pleistocene transition, this interval contains the shift in ice age cycles, that lengthened from ~ 40 to ~100 kyr, leading to warmer interglacial phases (Berger and Wefer, 2003; Jansen et al., 1986; Lisiecki and Raymo, 2005) and glacial terminations of greater amplitude (Terminations I–V; Past Interglacials Working Group of PAGES, 2016) than before. Among the other interglacial periods of the Mid-Brunhes, MIS 11 (424-374 kyr; Lisiecki and Raymo, 2005) has been proposed as a model to analyse the natural climate variability for several reasons: (i) the intensity and duration of the warming (Bauch et al., 2012; Hodell et al., 2000; PAGES, 2016); (ii) the enhanced penetration of the warm waters poleward (Berger and Wefer, 2003); and (iii) the increase in atmospheric greenhouse gas concentrations (Raynaud et al., 2005; Yin and Berger, 2012). All these processes are considered as main drivers of the collapse of the Greenland and west Antarctica ice sheets, and resulted in the eustatic sea-level rising about 20 m higher than it currently is (Olson and Hearty, 2009; Raymo and Mitrovica, 2012; Reyes et al., 2014; Roberts et al., 2012). Termination V, at the MIS 12/MIS 11 transition (424 kyr; Lisiecki and Raymo, 2005), is furthermore regarded as the largest amplitude glacial/interglacial transition of the last 800 kyr (PAGES, 2016).

MIS 11 is often considered a potential analogue for the Holocene as there are multiple similarities between both intervals, including: (i) the similar orbital forcing parameters of low eccentricity, high obliquity, low precessional amplitude, and insolation geometry (Berger and Loutre, 1991; Loutre and Berger, 2003); (ii) the elevated atmospheric CO_2 levels (Droxler and Farrell, 2000); and (iii) a small amount of continental ice (Loutre and Berger, 2003) similar to present conditions (Candy et al., 2014; Rohling et al., 2010; Yin and Berger, 2012).

Several paleoclimate records evidence the prevalence of long-lasting (~30 kyr) warm and stable conditions during the early substage of the full interglacial, MIS 11c period (Desprat et al., 2007; Martrat et al., 2007; McManus et al., 2003; Oppo et al., 1998; Stein et al., 2009; Voelker et al., 2010). Nevertheless, mid-latitude terrestrial climate-records indicate contrasting early climate instabilities during MIS 11c on centennial (Koutsodendris et al., 2010; Prokopenko et al., 2010; Tye et al., 2016) to millennial time-scales (Oliveira et al., 2016; Tzedakis et al., 2009), keeping the discussion open regarding the homogeneity of the latitudinal extent of the full interglacial conditions. Suborbital-scale climate instabilities are comparatively well recorded during MIS 11 b and MIS 11a (~395-374 kyr), in the North Atlantic to the Iberian latitudes (de Abreu et al., 2005; Hodell et al., 2013; Martrat et al., 2007; Palumbo et al., 2013; Rodrigues et al., 2011; Stein et al., 2009; Voelker et al., 2010) and the western Mediterranean (Marino et al., 2018). The origin of these instabilities has been associated with the southward incursion of waters with an Arctic origin (e.g. Oppo et al., 1998), and their effect on weakening the North Atlantic Meridional Overturning Circulation and coupled atmospheric interactions (Barker et al., 2015; McManus et al., 2003).

The Alboran Sea is the westernmost basin of the Mediterranean Sea, and hence, it has a crucial role in forming climate connections with the North Atlantic (Cacho et al., 1999, 2000; Martrat et al., 2004; Sierro et al., 2005). The Alboran Sea thus represents a strategic location for the reconstruction of palaeoceanographic and paleoclimatic variability for the whole Mediterranean Basin (e.g., Ausín et al., 2015a,b; Bazzicalupo et al., 2018; Colmenero-Hidalgo et al., 2004). Currently, the variability in sea-level, temperature, and precipitation in the region is partially controlled by fluctuations in the atmospheric gradient between the Azores High-pressure (AH) and the Icelandic Low-pressure (IL) cells, which constitutes the North Atlantic Oscillation mode (NAO) of winter climate variability in the North Atlantic region (Hurrell, 1995; Lionello, 2012). The changing NAO-*like* phase has been identified as a triggering mechanism for paleoenvironmental oscillations in the western Mediterranean during the Holocene (Fletcher et al., 2013; Frigola et al., 2007), with effects on primary productivity in the Alboran Sea (e.g., Ausin et al., 2015b; Bazzicalupo et al., 2020).

The sensitivity of coccolithophores to the changing surface ocean physicochemical conditions (temperature, salinity, nutrient-concentrations, and turbulence) makes them a valuable tool for the reconstruction of rapid palaeoceanographic fluctuations (Baumann et al., 2005). The high accumulation rate and adequate preservations of nannofossil (calcite plates termed coccoliths) in sediments throughout the Atlantic and Mediterranean Iberian margins have allowed for a number of studies, revealing the strong dependence of the coccolithophore primary productivity and assemblage-structure on the global climate at orbital and suborbital/millennial-scale (Amore et al., 2012; Ausín et al., 2015a,b; Bazzicalupo et al., 2018; Colmenero-Hidalgo et al., 2004; Marino et al., 2018; Palumbo et al., 2013).

The main objective of the present study was the high-resolution reconstruction of environmental and climatic changes in the Alboran Sea during the MIS 12/MIS 11 transition and MIS 11. Considering the coccolithophore primary productivity patterns as a proxy to monitor the changes in the surface and subsurface water column conditions, we attempted to unravel the past variations in the oceanographic circulation and its atmospheric configuration forcing at the western Mediterranean region. We integrated the high-resolution coccolithophore primary productivity record –inferred from the nannofossil characterization and quantification–, with the high-resolution records of the stable δ^{18} O and δ^{13} C isotopes from the planktonic foraminifera *Globigerina bulloides* and the alkenone $U^{k'}_{37}$ Sea Surface Temperatures (SST) at Ocean Drilling Program (ODP) Site 977. Additionally, the record of the opal phytolith content at ODP Site 977 together with the Mediterranean forest pollen taxa at the Portuguese Iberian margin Integrated Ocean Drilling Program (IODP) Site U1385 from Oliveira et al. (2016), were used to reconstruct the response of the Alboran Sea to atmospheric precipitation and wind track configuration during the MIS 12/MIS 11 transition and MIS 11 and their connections with the paleoclimate and palaeoceanographic processes of the North Atlantic.

2. The Alboran Sea

2.1. Oceanographic and atmospheric setting

ODP Site 977 is located in the Alboran Sea, a transitional area between the semi-enclosed Mediterranean Sea and the adjacent Atlantic Ocean. As such, the circulation in this region is intense and characterized by an anti-estuarine model, with surface inflow of relatively low saline waters from the Atlantic (Atlantic Water, AW), and the outflow in depth of highly saline Mediterranean waters (Mediterranean Outflow Water, MOW) through the narrow and shallow Strait of Gibraltar (Pistek et al., 1985). The eastern branch of the Azores Current (AzC; Johnson and Stevens, 2000) is the main source of the AW that flow into the Alboran Sea as a strong Atlantic Jet (AJ) though the upper ~200 m of the water column (Lafuente et al., 2000). The confluence of the Atlantic and Mediterranean waters results in the formation of two quasi-permanent anti-cyclonic gyres: the Western and Eastern anti-cyclonic Alboran Gyres (WAG and EAG, respectively; Heburn and La Violette, 1990. Fig. 1a). These gyres mix in the upper 300 m of the water column, resulting in pronounced variations in temperature, salinity, and nutrient distributions (Modified Atlantic Water, MAW).

The development, extension, and position of these hydrological

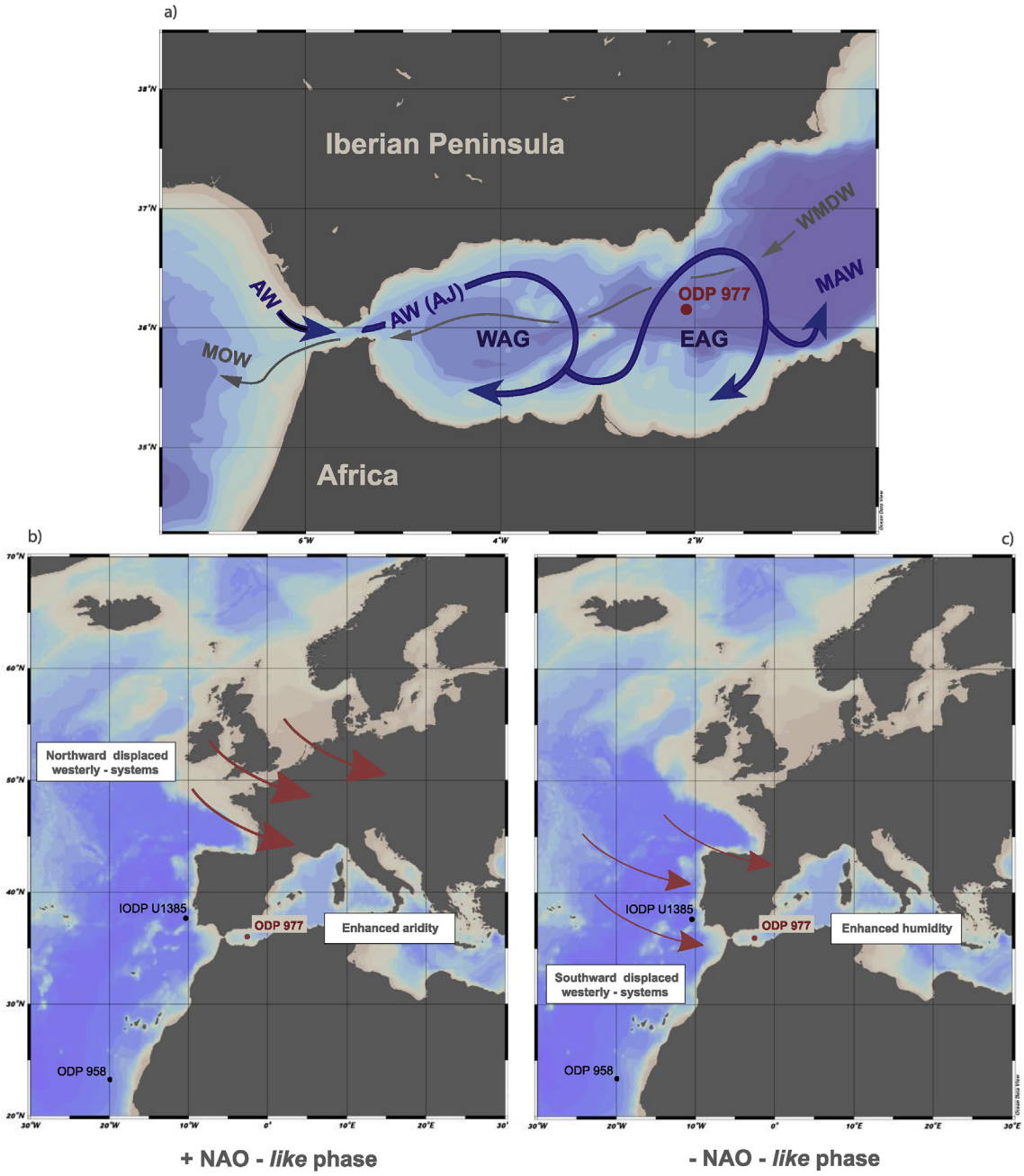

Fig. 1. **(a)** Geographic location and modern oceanographic circulation scheme of the study area. Arrows indicate the theoretical trajectories of water masses. Blue lines represent the surface circulation. Grey lines trace the circulation at depth. AW (Atlantic Water); MOW (Mediterranean Outflow Water); MAW (Modified Atlantic Water); WAG (Western Alboran Gyre); EAG (Eastern Alboran Gyre); WMDW (Western Mediterranean Deep Water). **(b)** and **(c)** Schematic NAO-*like* phase scenarios that synthetize the main processes controlling the activation of the *Alboran Upwelling System* during **(b)** + NAO-*like* phase and **(c)** − NAO-*like* phase. Location of ODP Site 977 (red dot, this study) and the IODP Site U1385 and ODP Site 958 (black dot) discussed in the text. (For interpretation of the references to colour in this figure legend, the reader is referred to the Web version of this article.)

structures is unstable and highly variable (Heburn and La Violette, 1990; Perkins et al., 1990). In the deeper layers of the water column (>300 m), the dense MOW, which is a mixture of Levantine Intermediate Water (LIW) and Western Mediterranean Deep Water (WMDW), exits the Strait of Gibraltar, flowing into the Atlantic and forming a distinct water mass whose imprint can be identified in much of the North Atlantic (Millot et al., 2008).

The climatic seasonality of the western Mediterranean is influenced by the Azores atmospheric high-pressure cell, resulting in warm-dry summers and mild-humid winters (Quézel and Médail, 2003; Sarnthein et al., 1982; Sumner et al., 2001), which control the wind circulation/intensities and the moisture availability (Lionello, 2012). At decadal and longer timescales, the climate variability in the Mediterranean and the North Atlantic region is triggered by the winter atmospheric pressure gradient between the Azores High (AH) and the Iceland Low (IL) systems, which defines the North Atlantic Oscillation (NAO; Hurrell et al., 1995). Currently, the fluctuations in the NAO phase largely modulate the position and strength of the westerlies, the seasonal mean heat and moisture transport over the ocean and the path and frequency of storms. They can also be responsible for important changes in ocean temperature and sea-ice cover in the Arctic region (Hurrell, 1995; Trigo

et al., 2002). In the modern Mediterranean, a positive (+) phase of the NAO (Fig. 1b) leads to drier and cooler conditions during the winter, due to a northward positioning of the westerly and northwesterly winds and storm tracks over the northern European latitudes. In contrast, the negative (−) phase of the NAO (Fig. 1c) generates wetter and warmer winter conditions over the Mediterranean, caused by the weakening and southward positioning of the westerly and northwesterly systems and storm tracks across the North Atlantic (Dai et al., 1997; Hurrell, 1995; Rodó et al., 1997). These winter anomalies are involved in deep-water convection and WMDW formation in the Northwestern (NW) Mediterranean (Millot, 1999) and the net water influx across the Strait of Gibraltar (Fenoglio-Marc et al., 2013); mechanisms that ultimately control the intensity of the circulation in the Alboran Sea (Pistek et al., 1985).

2.2. The Alboran Upwelling System

The Mediterranean Sea is classified as an oligotrophic basin, owing to its extremely low nutrient concentrations that limit phytoplankton growth. There are, however, a few regions with high algal biomass accumulations, including the Alboran Sea (see Siokou-Frangou et al., 2009 for a review). In the Alboran Sea, vertical mixing is the main mechanism fuelling phytoplankton production (Packard et al., 1988). The two main upwelling mechanisms in operation are: (i) the offshore upwelling associated with the formation of the two Alboran gyres, which is mainly controlled by the intensity of the AJ (Garcia-Gorriz and Carr, 1999; Sarhan et al., 2000); and (ii) the wind-induced coastal upwelling in the north western Alboran Sea, driven by the westerly winds blowing along the southern Iberian coast (Parrilla and Kinder, 1987). These mechanisms are referred to hereinafter as the *Alboran Upwelling System*. The intensity of this system and, consequently, the phytoplankton distributions in the Alboran Sea, are ultimately dependent on atmospheric circulation over the western Mediterranean (d'Ortenzio and Ribera d'Alcalà, 2009; Garcia-Gorriz and Carr, 1999; Lafuente et al., 2000).

In the Alboran Sea, the strong wind force and decrease in solar irradiance during the winter results in a replenishment of nutrients in the surface layer, favouring a spring peak of primary productivity and coccolithophore export to deeper levels, as documented in other Mediterranean regions of high productivity such as the NW Mediterranean (d'Ortenzio and Ribera d'Alcalà, 2009; Rigual-Hernández et al., 2013). Nevertheless, exceptional production during anti-cyclonic conditions over the region suggests that the surface Atlantic flux plays a major role in the stimulation of phytoplankton blooms (d'Ortenzio and Ribera d'Alcalà, 2009). The incoming AW not only introduces high amounts of nutrients, but is also responsible for the eastward transport and distribution of biogenic materials produced in the westernmost sector of the basin (Garcia-Gorriz and Carr, 1999; Salat and Cruzado, 1981).

3. Material and methods

3.1. Site location and core materials

ODP Site 977 is located in the eastern basin of the Alboran Sea (36° 1.9′N, 1° 57.3′W; Figs. 1), 1984 m below sea level. The sediment composition of the studied interval corresponds to 67.49–58.64 corrected meters below sea floor (cmbsf) from cores 8 and 7 of hole 977 A. The correction was made to adjust the 10.01 and 10.03 m of recovery, respectively in core 8 and 7, to the standard core length of 9.5 m.

The core materials are composed by an open marine-hemipelagic facies of nannofossil-rich to calcareous silty clay, with $CaCO_3$ content varying between 43.2 and 57.7 wt % (Comas et al., 1996).

3.2. Coccolith sample preparation and analysis

A total of 181 samples for the coccolithophore analyses were selected, each at 4–6 cm spacings from the hole 977 A. Slides for nannoplankton analysis were prepared following the random settling technique outlined by Flores and Sierro (1997). Coccolith identification and counting were carried out using a cross polarized-light Nikon Eclipse *80i* petrographic microscope at 1000× magnification. All slides were analysed by counting a minimum of 400 coccoliths in a variable number of fields of view. A second supplementary count of 10 fields of view was performed to accurately determine the abundance of the rarer taxa. Reworked nannofossils were counted separately and expressed as absolute concentrations, (N), and as a percentage of the total concentration. A semiquantitative estimation of the coccolith preservation was applied using the scanning electron microscope (SEM) visual observation and following the scale established by Flores and Marino (2002).

A total of 21 taxa were recognized. Identification of the coccolithophore species followed Young et al. (2003), and the guide to the biodiversity and taxonomy of coccolithophores Nannotax 3 (ina.tmsoc.org/Nannotax3/index.html). Further considerations were made for the *Gephyrocapsa* specimen classification, following Flores et al. (2000). Only mid-sized specimens (3–4.5 μm) with closed or very small central openings were considered as *Gephyrocapsa caribbeanica*; all the *Gephyrocapsa* individuals that were <3 μm, with both open and closed central openings, were grouped as 'small *Gephyrocapsa*'. *Oolithotus* spp., *Umbilicosphaera sibogae*, *Umbilicosphaera foliosa* (both as *Umbilicosphaera* spp.), *Rhabdosphaera clavigera*, *Umbellosphaera* spp., and *Calciosolenia* spp. were lumped together in the Warm Water Taxa (WWT) group. *Coccolithus pelagicus* was subdivided into the subspecies *C. pelagicus* subsp. *pelagicus* (5–10 μm), *C. pelagicus* subsp. *braarudii* (<13 μm), and *C. pelagicus* subsp. *azorinus* (15–16 μm) (Geisen et al., 2002; Parente et al., 2004).

3.3. Coccolithophore paleoenvironmental considerations

Variations in the coccolith abundances were estimated using percentages, coccolith absolute values (N) and nannofossil accumulation rates (NAR). N and NAR were calculated according to Flores and Sierro (1997) (Fig. 3c and d). For NAR calculations, the bulk density was obtained from the gamma-ray attenuation density (Comas et al., 1996), and the linear sedimentation rates were calculated from the age model (Fig. 3a). NAR is considered to be an estimate of paleoproductivity (Steinmetz, 1994; Baumann et al., 2004), as it depends on the surface water conditions controlling the proliferation of coccolithophores (Flores et al., 1997; Baumann et al., 2005; Stolz and Baumann, 2010). Following previous studies in the region (Colmenero-Hidalgo et al., 2004; Ausín et al., 2015a,b), these parameters were considered indicators of the coccolithophore primary productivity variability through time.

Eutrophic conditions in the upper photic zone are known to favour coccolithophore proliferation (Barber and Hiscock, 2006; Baumann et al., 2005), in particular the r-selected coccolithophore species, such as those belonging to the *Gephyrocapsa* genus (Young et al., 2000). The small *Gephyrocapsa* group refers to a cluster of opportunistic species dwelling in the uppermost photic zone (Gartner, 1988; Takahashi and Okada, 2000), with affinity for strong vertical mixing, and surface eutrophication in the Alboran Sea

(Hernández-Almeida et al., 2011; Knappertsbusch, 1993). *G. caribbeanica* dominates the coccolith fossil assemblages during the interglacial stages of the Mid-Brunhes interval, including the MIS 11 (e.g., Amore et al., 2012; Marino et al., 2014), although its nature and ecological roles are debated (Bollmann et al., 1998; Flores et al., 2012). Due to the cosmopolitan distribution of *G. caribbeanica*, the ecology of this species is considered analogous to the modern *Emiliania huxleyi* (e.g., Saavedra-Pellitero et al., 2017) and, therefore its N values are grouped together with those of the small *Gephyrocapsa* in the primary productivity proxy (PPP; Fig. 3f). The PPP is used to trace the activation of the *Alboran Upwelling System*, increasing the accuracy of the net coccolithophore primary productivity signal by removing the load of minor species not completely related to the autochthonous coccolith production at the Alboran Sea. Proportions of small *Gephyrocapsa* up to the threshold of 40% are interpreted as intensified activation of the *Alboran Upwelling System*, following the observations by Bárcena et al. (2004) during pronounced active upwelling periods in the region inferred from sediment trap records.

The coccolithophore temperature-sensitive assemblage refers to species with ecological requirements associated with a specific temperature range. For instance, the presence of the subpolar water taxon *C. pelagicus* subsp. *pelagicus* is interpreted as a tracer of pulses of polar/subpolar water inflow into the Iberian latitudes (e.g., Amore et al., 2012; Marino et al., 2018; Marino et al., 2014). The tropical/subtropical species composing the WWT group have a common ecological affinity for tropical-subtropical surface waters (Baumann et al., 2004; Boeckel and Baumann, 2004; Winter 1994). The presence of WWT in living and Holocene coccolith assemblages in the Mediterranean is scarce (Knappertsbusch, 1993). Therefore, an increased abundance of these species in our record is considered as a proxy of the enhanced influence of the warm AzC current across the Strait of Gibraltar.

3.4. Opal phytolith analysis

Opal phytoliths are siliceous biogenic particles formed in the aerial tissues of plants, and are particularly abundant and characteristic of the Poaceae family (Carter and Lian, 2000; Twiss, 1992). Since there are no important river systems in the region, the phytolith content in the Alboran Sea is considered to be a wind-transported microfossils that are likely to be sourced from North Africa (Bárcena et al., 2001 and references therein). During periods of dry conditions and marked seasonality over the NW African region, large amounts of phytoliths from tall-grass savannah produced during the humid season are injected into the atmosphere (Flores et al., 2000). The phytolith profile in the Alboran Sea is thus considered to trace the more arid conditions and intensified winds from North Africa.

A set of 35 samples from the hole 977 A were analysed for the content of opal phytolith particles in the sediments. Samples were prepared according to the randomly distributed method outlined in Bárcena and Abrantes (1998). Several transects, accounting for a total surface of 8 mm^2 per slide, were studied. Quantitative analyses were performed at 1000 $\times$, using a Leica DMLB with phase-contrast illumination. The absolute values are expressed as the number of phytoliths per gram (phytolith g^{-1}; Fig. 6f).

3.5. Stable isotopes

The Stable isotope analyses were carried out in 272 samples from 977 A at intervals of 2–5 cm. A number of 11 hand-picked specimens of *Globigerina bulloides* per sample were measured. The individuals were separated from the >300 μm size fraction and crushed and cleaned with methanol and ultrasonicated for a few minutes. The $\delta^{18}O$ and $\delta^{13}C$ measurements were performed on an IRMS (isotope-ratio mass spectrometry). Finnigan-MAT 252 coupled to a single acid bath CarboKiel-III carbonate preparation device at the Scientific and Technological Centre of the University of Barcelona (CCiT-UB). Analytical uncertainties were obtained by means of an in-house carbonate standard that is calibrated to NBS-19 international standard (Coplen, 1996). The uncertainties were 0.04‰ VPDB for $\delta^{13}C$ and 0.08‰ VPDB for $\delta^{18}O$.

3.6. Alkenone $U^{K'}_{37}$ for SST reconstruction

Biomarker extraction was carried out on the same samples selected for coccolithophore analysis following the protocol described by Villanueva et al. (1997). An internal standard (n-nonadecan-1-ol, n-hexatriacontane and n-dotetracontane) was added to about 2.5 g of sediment, which was extracted with dichloromethane in an ultrasonic bath. The extracts were saponified with 10% KOH in methanol. The extraction of the neutral lipid fraction was performed with the use of hexane and dried under a gentle flow of nitrogen. After that, toluene solvent was used to re-dissolve and the compounds were derivatized with bis(-trimethylsilyl)trifluoroacetamide. The gas chromatography analysis was carried out on a Varian 3800 equipped with a CPSIL-5 CB column coated with 100% dimethylsiloxane (film thickness 0.12 mm) using hydrogen as carrier gas (50 cm/s). Analytical errors were <10% and the uncertainty in the $U^{K'}_{37}$ determinations lower than 0.015 (ca. $\pm$ 0.5 °C). The complete procedure and analysis were performed at the department of environmental chemistry (IDAEA-CSIC) of Barcelona.

The $U^{K'}_{37}$ index (Brassel et al., 1986; Prahl and Wakeham, 1987) was calculated after quantification of [$C_{37:2}$], that indicates the concentration of (E,E)-15,22-heptatriacontadien-2-one and [$C_{37:3}$], referred to the concentration of (E,E,E)-8,15,22-heptatriacontatrien-2-one. The values were converted into Sea Surface Temperatures (SST) using a calibration equation from sediment samples and annual average SST of overlying waters (Müller et al., 1998).

4. Results

4.1. Chronological framework

The chronology of the sediments was established by correlating the SSTs of both ODP Site 977 and the North Atlantic mid latitude IODP Site U1313 (Stein et al., 2009), for which the available age model is based on the correlation of the benthic $\delta^{18}O$ with the global LR04 stack (Voelker et al., 2010). As the SST at Sites 977 and 1313 is controlled by the Azores Current, we assumed that there would be synchronous variations. The adjustments for the studied interval were made by including five primary control points (Fig. 2 Table 1), while the age of each sample was calculated using linear interpolations between the age control points.

The studied interval spans were from 429.7 kyr at the MIS 12/MIS 11 transition to 376.3 kyr, near the isotopically MIS 11/MIS 10 boundary (Lisiecki and Raymo, 2005). The nomenclature of Railsback et al. (2015) was used for the identification of substages MIS 11c, 11 b, and 11a over the $\delta^{18}O$ *G. bulloides* of ODP Site 977 (Fig. 3h).

The high temporal resolution of the coccolithophore record, ranging between 0.02 and 0.3 kyr, provides an exceptional opportunity to reconstruct the environmental conditions in the Alboran Sea at a millennial to centennial scale.

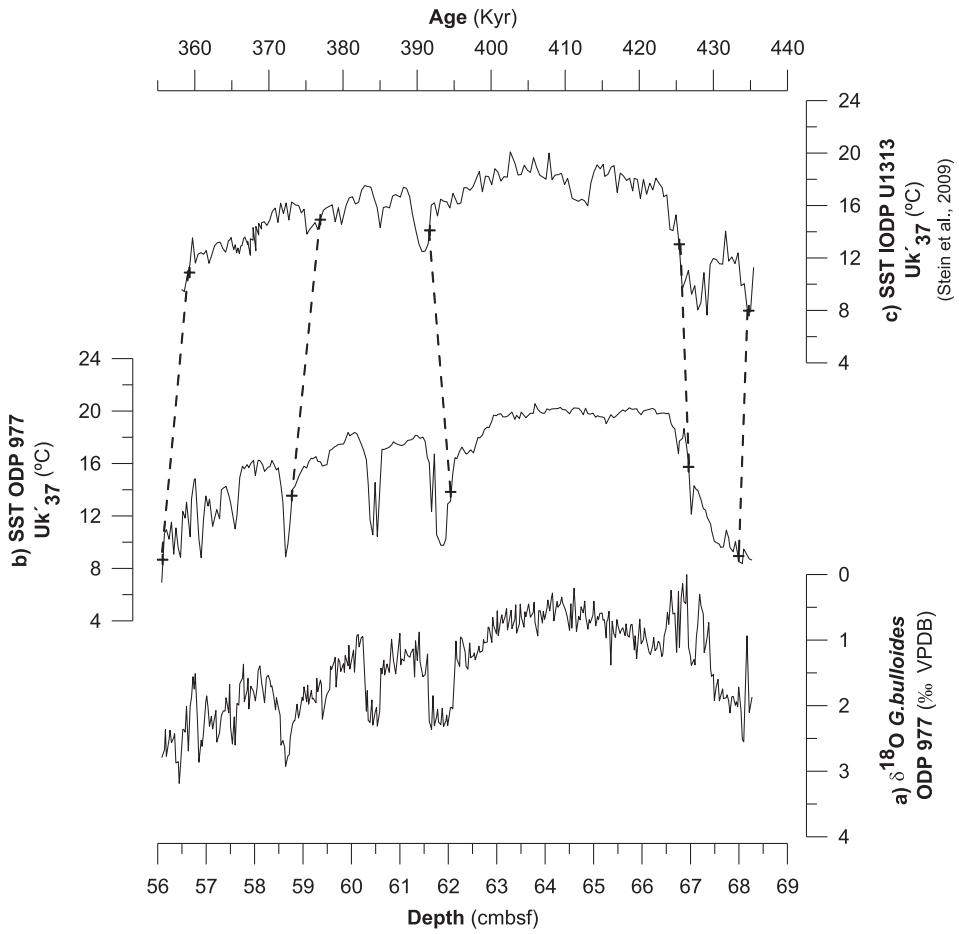

Fig. 2. Chronological framework of the studied materials. In depth scale **(a)** planktonic foraminifera $\delta^{18}O$ (‰ VPDB) from *G. bulloides* at ODP Site 977 and **(b)** $U^{k'}_{37}$ Sea Surface Temperature (SST) at ODP Site 977. In age scale **(c)** $U^{k'}_{37}$ SST at Site U1313 by Stein et al. (2009). Age assignment from correlation of the changes in SST at Site 977 with SST at Site U1313 (Stein et al., 2009). Control points used for the correlation are identified with the dashed lines.

4.2. Coccolithophore assemblages

Species of the genus *Gephyrocapsa* dominated the coccolithophore assemblages during the entire analysed interval (Fig. 4). The small *Gephyrocapsa* group and *G. caribbeanica* are the major contributors, accounting respectively for 46 and 20% of the average relative abundances (Fig. 4c and d). The proportion of the small *Gephyrocapsa* group was over the threshold of 40% at the MIS 12/MIS 11 transition (429.7-418 kyr), during the late MIS 11c (from 405 kyr), and between 396-388 kyr and 385-376 kyr during the MIS 11 b and MIS 11a (Fig. 4c). The proportion of *G. caribbeanica* was over 30% during the MIS 11c (420-400 kyr), and between 389-384 kyr and 383-380 kyr within MIS 11 b (Fig. 4d). The average contribution of *G. oceanica* was ~16%, displaying values over 20% from 405 kyr, during the late MIS 11c and MIS 11 b (Fig. 4e). *G. muellerae* is the least abundant *Gephyrocapsa* species, averaging 3% (Fig. 4f). Increased percentages are recorded during the MIS12/MIS11 transition (430-422 kyr), briefly at 384 kyr within MIS 11 b, and from 378 kyr within MIS 11a (Fig. 4f).

The WWT % increases during the MIS12/MIS11 transition (426–423.5 kyr) and within the late MIS 11c (412–392.5 kyr; Fig. 5c). *C. pelagicus* subsp. *pelagicus* is scarcely recorded at MIS 11c (until 413.5 kyr) and around 391 and 385 kyr during MIS 11 b (Fig. 5d). The abundance of *Helicosphaera carteri* and *Syracosphaera* spp. increases at the end of the MIS 12/MIS 11 transition and from 405 kyr, during the late MIS 11c and MIS 11 b (Fig. 5e and f). *C. pelagicus* subsp. *azorinus* increases its numbers during MIS 11 b (from 397 kyr; Fig. 5g). Reworked nannofossils are present in low proportions over the complete studied period (Fig. 3e). The highest percentages are registered at MIS 11c until 414 kyr, and secondary maxima are observed at 391 and 385 kyr within MIS 11 b (Fig. 3e).

4.3. Coccolith absolute values and primary productivity proxy

The preservation of coccoliths in samples is good. The absence of dissolution affecting the nannofossil concentration in samples is further in favour of the usefulness of N as a reference of the coccolithophore primary productivity across the interval. The average of the total N ranged between 10×10^9 and 60×10^9 coccoliths g^{-1} (Fig. 3c). Enhanced PPP values above the threshold of 20×10^9 coccoliths g^{-1} were observed between 428 and 422 kyr during the MIS 12/MIS 11 transition, between 405 and 397.5 kyr in the late MIS 11c, and during three short intervals at 397.5–392 and 388-386 kyr in MIS 11 b and at 382-376 kyr in MIS 11a (Fig. 3f and 6c). The lowest recorded PPP were during the early MIS 11c (422-405 kyr) and two abrupt drops centred at ~390 and 383 kyr (Fig. 3f). Maximum values for the N of *G. oceanica* were recorded up to the late MIS 11c, and then there were three pulses of enhanced abundance around 396, 388, and 380 kyr (Fig. 4e and 6h). The highest N of *G. muellerae* occurs at the MIS 12/MIS 11 transition and MIS 11a (Fig. 4f).

The N values of the WWT increased during the final part of the

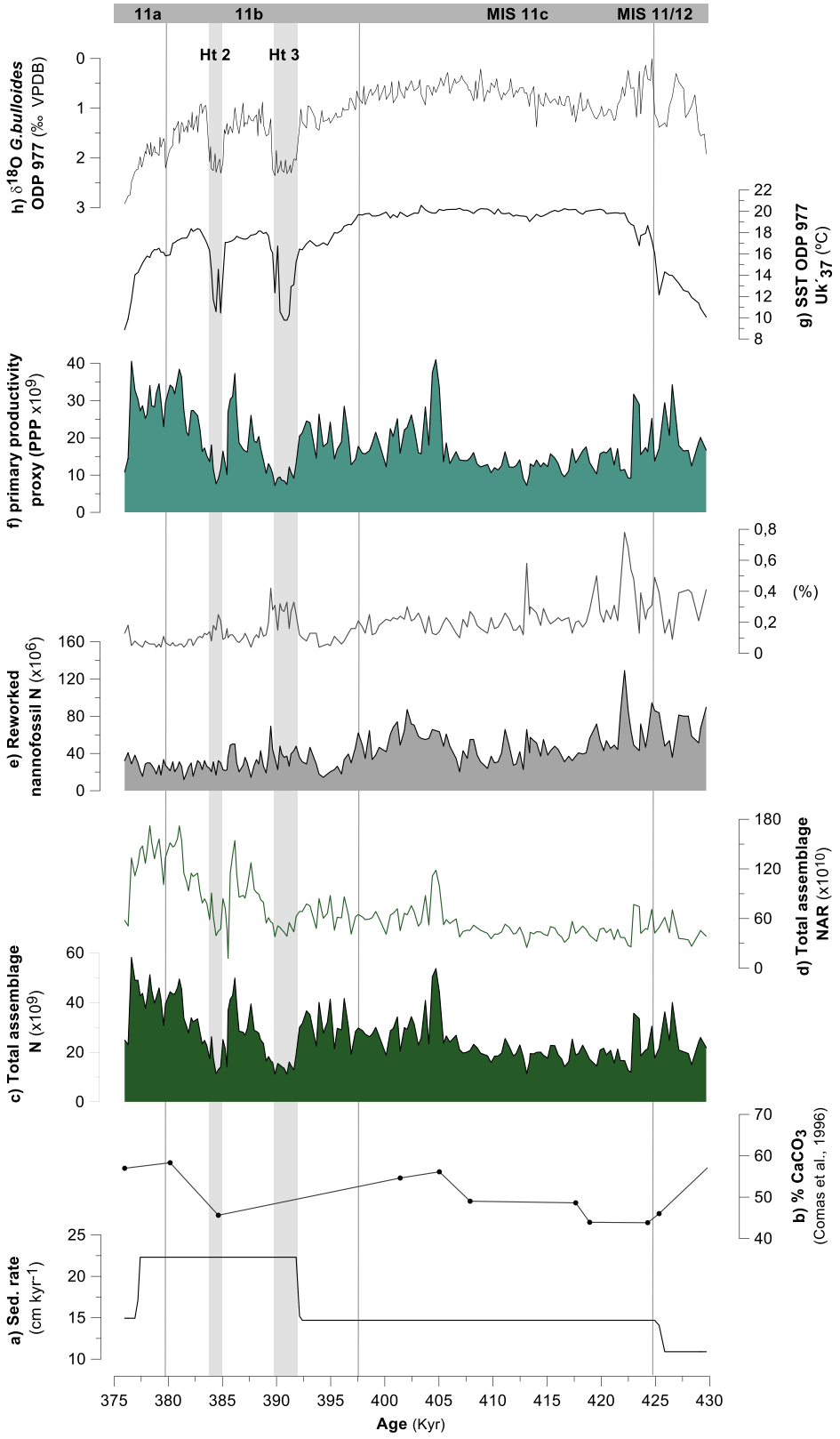

Fig. 3. Characterization of the calcareous nannofossil content in the sedimentary record: **a)** Sedimentation rate (cm kyr^{-1}); **b)** carbonate content (% $CaCO_3$) from Comas et al. (1996); **c)** number of coccoliths per gram of sediment (N; [coccolith g-1]) of the total assemblage; **d)** Nannofossil Accumulation Rates (NAR; [coccolith cm^{-2} kyr^{-1}]) of the total assemblage; **e)** Reworked nannofossils as absolute values (N; [coccolith g^{-1}]) and relative abundance (%); **f)** primary productivity proxy (PPP = N small *Gephyrocapsa* + N *G. caribbeanica;* [coccolith g^{-1}]); **g)** $U^{k'}_{37}$ Sea Surface Temperature (°C) at ODP Site 977; **h)** planktonic foraminifera $\delta^{18}O$ (‰ VPDB) from *G. bulloides* at ODP Site 977. Substages are indicated according to Railsback et al. (2015). Grey bands represent the Heinrich-*type* events 3 and 2.

Table 1
Primary control points used to correlate the SST values at IODP Site U1313 (Stein et al., 2009) and ODP Site 977. Cmbsf: corrected meters below seafloor.

ODP Site 977 depth (cmbsf)	Age (kyr)	Sed. Rate (cm/kyr)
56.107	359.00	14.94
58.812	377.11	22.31
62.096	391.82	14.69
67.009	425.26	10.90
68.070	435	7.63

MIS 12/MIS 11 transition, and from 413 kyr during the late MIS 11c (Fig. 5c). *C. pelagicus* subsp. *pelagicus* exhibited a decrease in its N from the early MIS 12/MIS 11 transition, towards MIS 11c (Fig. 5d). The N of the *H. carteri* and *Syracosphaera* spp. exhibited high values at the MIS 12/MIS 11 transition and marked pulses of increased abundance during the late MIS 11c (Fig. 5e and f). *C. pelagicus* subsp. *azorinus* increased above the MIS 11 b/MIS 11c transition (Fig. 5g).

4.4. Phytolith content

The highest phytolith content (over 40×10^4 phytolith g^{-1}) was recorded at the MIS 12/MIS 11 transition (429.7-422 kyr), from the late MIS 11c to MIS 11c/MIS 11 b transition (at 407, 404, and between 397-393 kyr), during the Ht2 (~383 kyr), and the MIS 11a (~376 kyr) (Fig. 6f). The phytolith record displays low values between 420 and 408 kyr in the early MIS 11c, between 389 and 384 in MIS 11 b, and 382-378 kyr towards MIS 11a (Fig. 6f).

5. Discussion

5.1. Atmospheric control mechanisms on the Alboran Upwelling System

The recorded PPP values, ranging from 7×10^9 to 41×10^9 coccolith g^{-1} (Fig. 3f and 6c), are of similar or higher magnitude than those documented in the Alboran Sea during periods of enhanced primary productivity, such as the Holocene (e.g. Colmenero-Hidalgo et al., 2004; Ausín et al., 2015a,b). Thus, it can be concluded that MIS 11 was a period of high coccolithophore primary productivity, most likely owing to the complete development of the *Alboran Upwelling System* (Fig. 6c). This observation is in agreement with earlier work in the western Mediterranean (e.g., Girone et al., 2013; Marino et al., 2018), and in the Portuguese Iberian margin (e.g., Amore et al., 2012; Maiorano et al., 2015; Palumbo et al., 2013), that also described MIS 11 as an interglacial period of high primary productivity.

Notably, the high resolution of our analysis reveals substantial intra-interglacial fluctuations in coccolithophore productivity, within the overall highly productive conditions during the MIS 12/MIS 11 transition and MIS 11 (430−376 kyr). Our data suggest that these fluctuations are intimately related to changes in the regional atmospheric circulation. In the modern North Atlantic, the winter + NAO phase is associated with an intensification and northward positioning of the westerly and northwesterly systems, while the winter - NAO phase is related to the weakening of the northwesterly winds that are conveyed towards midlatitudes, leading to an increase in the precipitations in the Mediterranean region and North Africa (Hurrell et al., 1995).

Periods of increased PPP (Fig. 6c) and when the percentage of small *Gephyrocapsa* reached the 40% threshold (Fig. 6d), are associated with the intensification of the *Alboran Upwelling System* (Fig. 7a). These time intervals are coupled with the increased content of wind-transported phytoliths (Fig. 6f). We propose that + NAO-*like* conditions were dominant during these intervals of increasing winter pressure gradients, and thereby favouring the transport of dry winds from the North African region (i.e. Saharan dust transport; Moulin et al., 1997, Fig. 7a). This concept is supported by pollen records at the nearby IODP Site U1385 (Oliveira et al., 2016, Fig. 6g), that suggests Mediterranean forest contractions are consistent with the northward displacement of westerly wind system during + NAO-*like* phases. In turn, the low PPP (Fig. 6c) and the decreased proportion of small *Gephyrocapsa* (Fig. 6d), were determined to be caused by the moderate activation of the *Alboran Upwelling System* (Fig. 7b). These intervals are coupled with low phytolith content, owing to a stronger influence of moist air masses over the western Mediterranean (Fig. 6f; Fig. 7b). This idea is consistent with the expansion of the Mediterranean forest during these intervals, strongly suggesting a southward positioning of the westerly winds (Oliveira et al., 2016, Fig. 6g).

The variability of westerly and northwesterly wind systems over the NW Mediterranean has an impact on the thermohaline overturning systems in the western Mediterranean (Cacho et al., 2000; Millot, 1999; Moreno et al., 2002). WMDW convection takes place during winter when the dry and cold northwesterly winds intensify, inducing cooling and evaporation of the surface waters in the NW Mediterranean (Cacho et al., 2000; Fenoglio-Marc et al., 2013; Rogerson et al., 2012; Rohling et al., 1998). Increased winter pressure gradients associated with + NAO-*like* conditions (Fig. 7a) intensify these mechanisms and surface circulation systems (Cacho et al., 2000), ultimately inducing a more vigorous AJ flux in the western Mediterranean. These conditions most likely result in the complete gyre development and associated upwelling systems, thereby favouring a more intense activation of the *Alboran Upwelling System* (Fig. 7a). As a feedback mechanism, the complete WAG activity may increase the admixture and acceleration in the WMDW (Lafuente et al., 2000). The N values and percentages of *Gephyrocapsa oceanica* can be used as a tracer of the surface Atlantic waters in the region (Alvarez et al., 2010; Knappertsbusch, 1993; Bazzicalupo et al., 2018, 2020) (Fig. 6h). The reduced winter pressure during the - NAO-*like* phases (Fig. 7b) results in mild winter conditions and a consequent reduction in WMDW formation, exerting a slowdown in the western Mediterranean circulation and regional AJ intensities (Cacho et al., 2000). The incomplete development of the Alboran gyres (and associated upwelling cells) and the sole coastal wind-induced upwelling development, is considered to weaken the activation of the *Alboran System*, limiting the overall regional coccolithophore primary productivity (Fig. 7b).

In the following sections we provide a chronological description for our high-resolution signal and a detailed discussion of its relationship with such fluctuations in the Mediterranean atmospheric and oceanographic circulation patterns.

5.2. MIS 12/MIS 11 transition (Termination V)

Between 428 and 422 kyr, the high PPP and percentages of small *Gephyrocapsa* (Fig. 6c and d), together with the increased phytolith concentrations (Fig. 6f) and a reduction in Mediterranean forest pollen records at Site U1385 (Fig. 6g), suggests an intensification of the *Alboran Upwelling System* triggered by more intense trade winds, as a result of + NAO-*like* conditions. A latitudinal aridification affecting the western Mediterranean across deglaciation is in agreement with the dry and cold midland conditions of SW Iberia (Oliveira et al., 2016) and the iron-enriched sediments affected by the enhanced Saharan dust fluxes at ODP Site 958 off NW Africa (Helmke et al., 2008).

A northward shift of the temperate westerlies is more likely to have resulted in an intensified AJ inflow into the Alboran Sea, stimulating the *Alboran Upwelling System*. The increased

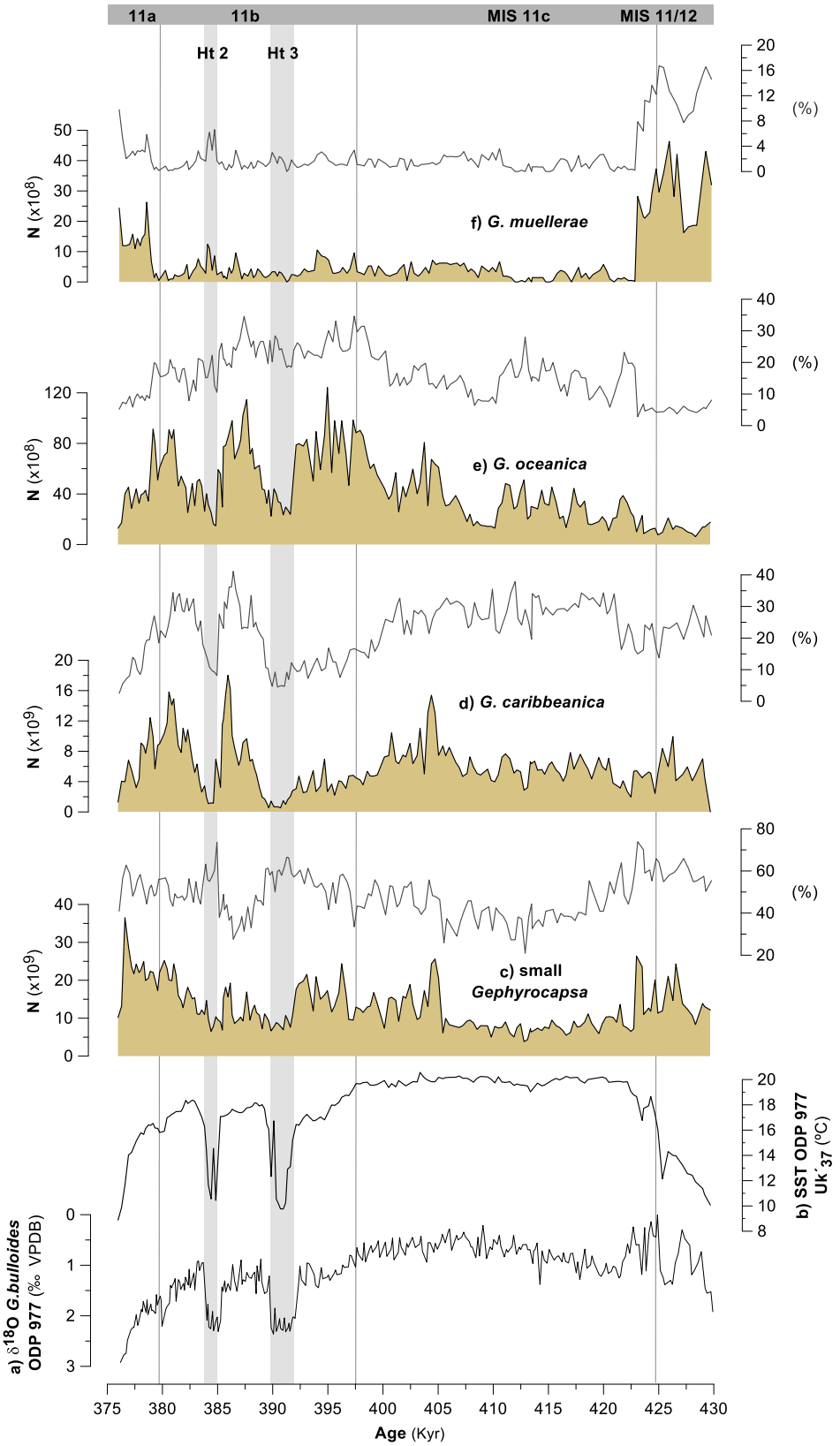

Fig. 4. Characterization of the major coccolithophore species of the assemblages during MIS 12/MIS11 and MIS 11 at ODP Site 977. **(a)** planktonic foraminifera $\delta^{18}O$ (‰ VPDB) from *G. bulloides* at ODP Site 977; **(b)** $U^{k'}_{37}$ Sea Surface Temperature (°C) at ODP Site 977. Absolute values (N [coccolith g-1]; filled areas) and relative abundances ([%]; grey lines) of **(c)** small *Gephyrocapsa* group; **(d)** *Gephyrocapsa caribbeanica*; **(e)** *Gephyrocapsa oceanica*; **(f)** *Gephyrocapsa muellerae.*

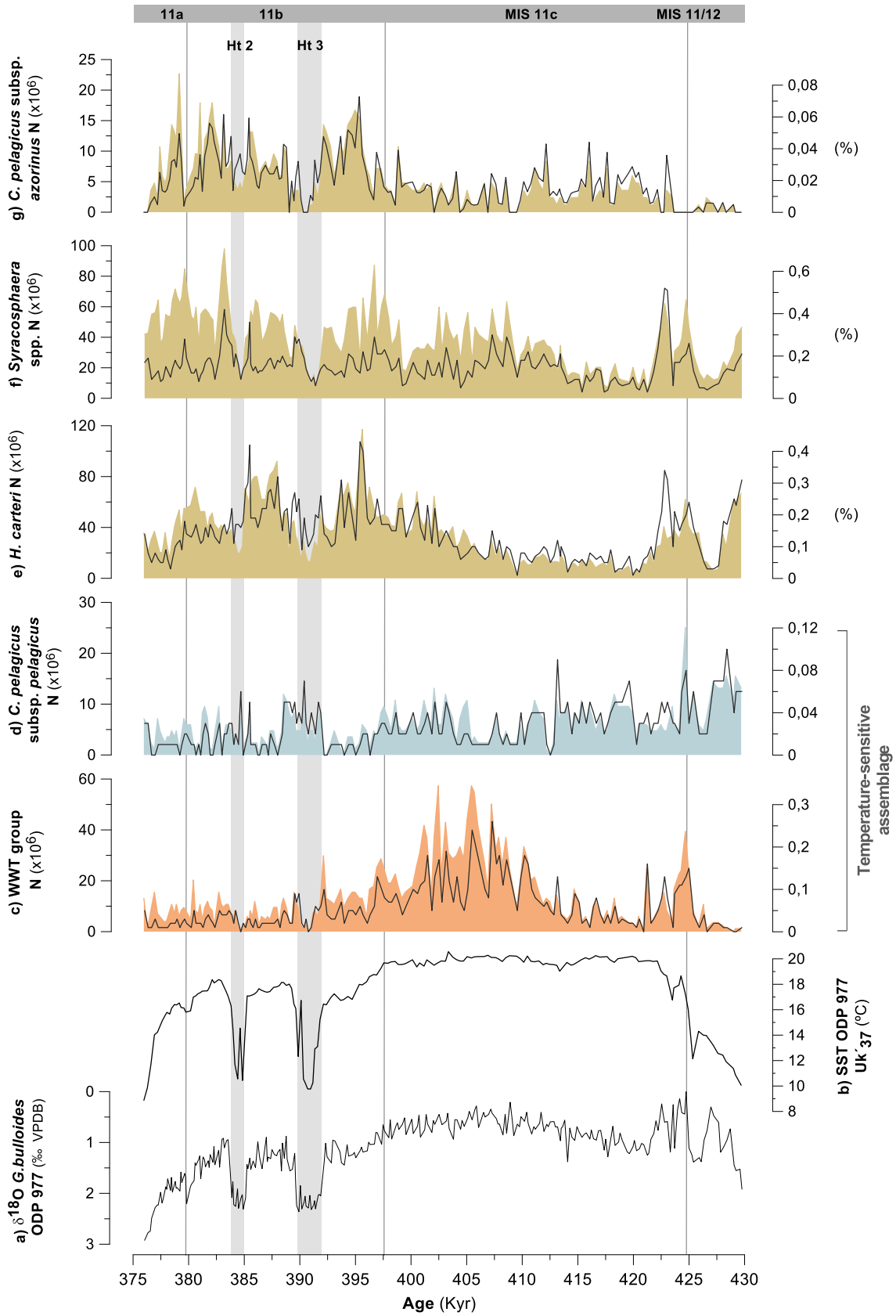

Fig. 5. Variations in the absolute abundance of minor coccolithophore species of the assemblages during MIS 12/MIS11 and MIS 11 at ODP Site 977. Absolute values (N [coccolith g^{-1}]; filled areas) and relative abundance ([%]; grey lines). **(a)** planktonic foraminifera $\delta^{18}O$ (‰ VPDB) from *G. bulloides* at ODP Site 977; **(b)** $U^{k'}_{37}$ Sea Surface Temperature(°C) at ODP Site 977; **(c)** Warm Water Taxa (WWT) group; **(d)** *Coccolithus pelagicus* subspecies *pelagicus* **(e)** *Helicosphaera carteri*; **(f)** *Syracosphaera* spp.; **(g)** *Coccolithus pelagicus* subspecies *azorinus*.

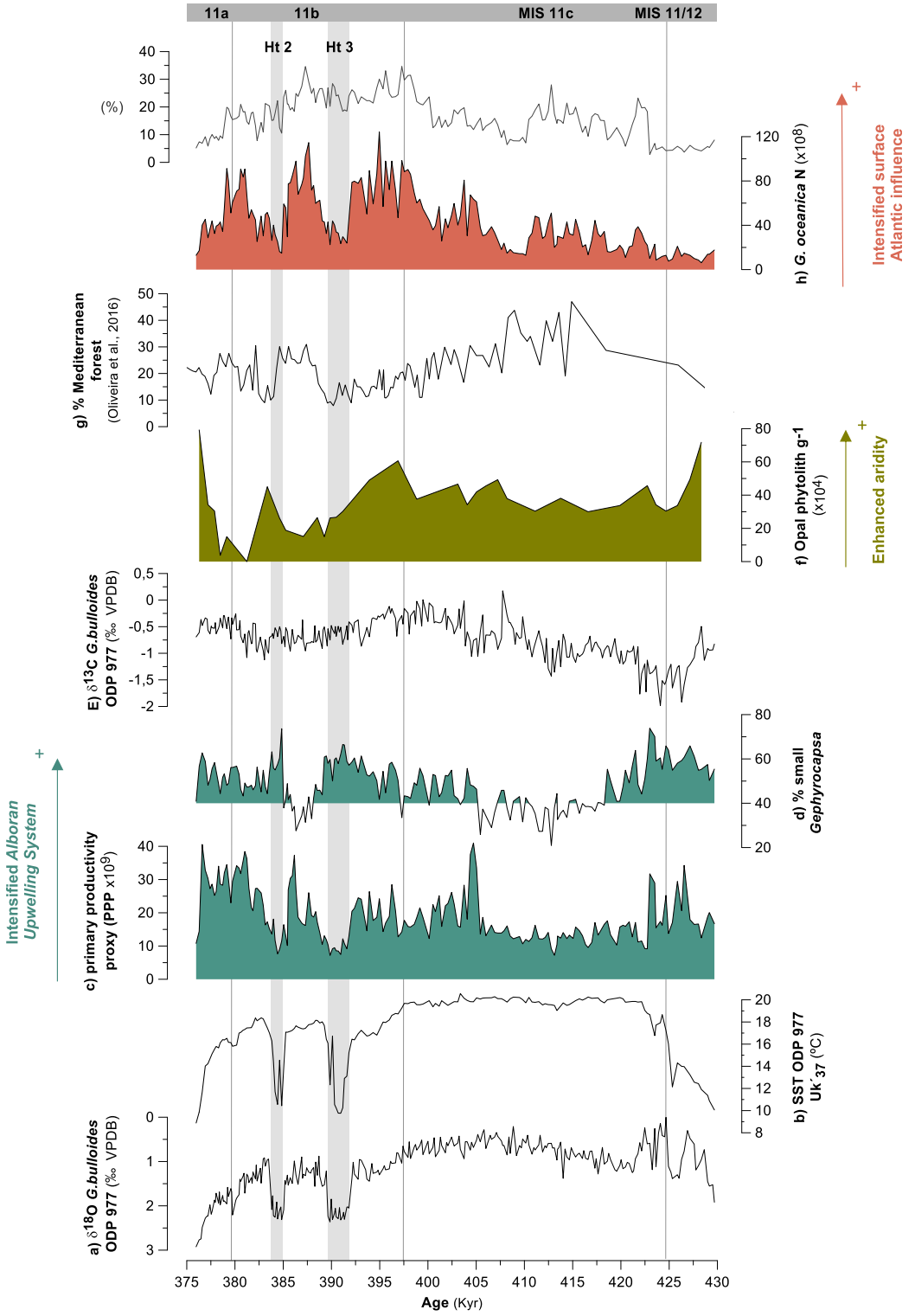

Fig. 6. Atmospheric and oceanographic proxies and their relationships with the *Alboran Upwelling System*. **(a)** $U^{k'}_{37}$ Sea Surface Temperature (°C) at ODP Site 977; **(b)** planktonic foraminifera $\delta^{18}O$ (‰ VPDB) from *G. bulloides* at ODP Site; **(c)** primary productivity proxy (N small *Gephyrocapsa* + N *Gephyrocapsa caribbeanica*; [coccolith g^{-1}]); **(d)** relative abundances (%) of small *Gephyrocapsa*; **(e)** planktonic foraminifera $\delta^{13}C$ (‰ VPDB) from *G. bulloides* at ODP Site 977; **(f)** Opal phytolith content at ODP Site 977 (phytolith g^{-1}); **(g)** relative abundances (%) of Mediterranean forest taxa at IODP Site U1385 (Oliveira et al., 2016); **(h)** absolute values (N [coccolith g^{-1}]) and relative abundances (%) of *Gephyrocapsa oceanica*.

concentration of reworked nannofossil during the MIS 12/MIS 11 transition (Fig. 3e) is tentatively suggested to be conditioned by depositional processes related to intensified deep circulation in the Alboran Sea. This idea agrees with a conspicuous MOW intensification during Termination V reported by Sánchez-Goñi et al. (2016). Timing of the restoration of the water exchange across the Strait of

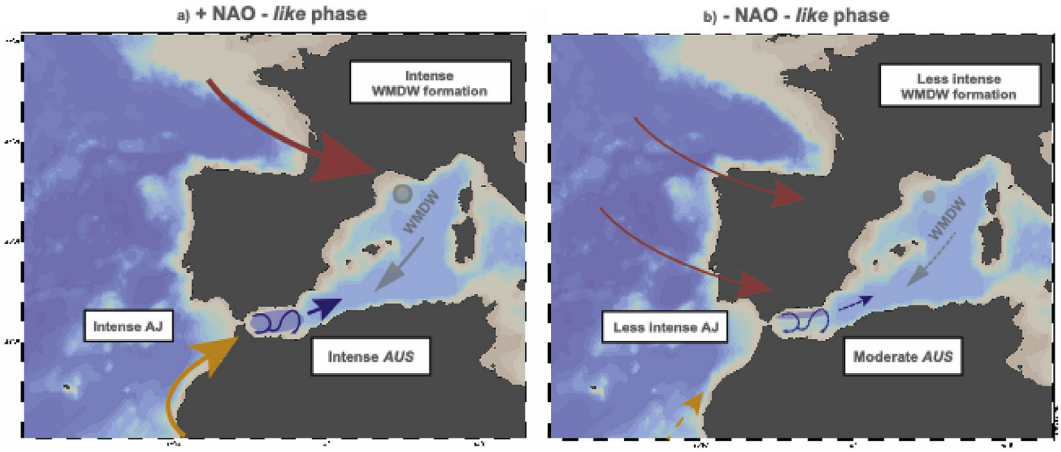

Fig. 7. NAO-*like* scenarios that summarize the main processes controlling the intensity of the *Alboran Upwelling System* and the coccolithophore primary productivity record during the MIS 12/MIS 11 and the MIS 11. AUS (*Alboran Upwelling System*); AJ (Atlantic Jet); WMDW (Western Mediterranean Deep Water).

Gibraltar during Termination V (Rohling et al., 1998, 2010) could contribute to the intensified AJ. In this sense, the intense surface influence of the AzC across the deglaciation promoting higher SST (Fig. 5b) is well identified by the increased percentages and N of the WWT group between 426 and 422 kyr (Fig. 5c). The coeval decrease in percentages and N of *G. muellerae*, associated with colder surface conditions in the region (Weaver and Pujol, 1988), evidences a reversal in the temperature-sensitive species comparable to that observed during the last glacial/interglacial transition of the Mediterranean (Incarbona et al., 2009).

Surface water nutrient-enrichment by the river discharges is not considered to be a regular factor controlling the regional primary productivity in the Alboran Sea (Sanchez-Vidal et al., 2005). Nonetheless, the higher abundances of *H. carteri* and *Syracosphaera* spp. (Fig. 5e and f), species which benefit from turbid, fresher, and productive surface conditions (Colmenero-Hidalgo et al., 2004; Giraudeau, 1992; Hernández-Almeida et al., 2011), suggest an exceptional continental discharge throughout the deglaciation. Nevertheless, the enhanced regional freshwater input due to the intensification of the surface Atlantic influence is regarded as the main driver of these processes.

5.3. MIS 11c

A moderate *Alboran Upwelling System* between 422 and 405 kyr of the early MIS 11c is recognized because of the lowered PPP and percentages of small *Gephyrocapsa* (Fig. 6c and d). Its control by -NAO-*like* configuration is suggested from the less intense wind supply from N Africa into the Alboran Sea and the consequent decrease in phytolith content (Fig. 6f) and the increased Mediterranean forest pollen record at Site U1385 (Fig. 6g). In line with this interpretation is the timing of changes leading to a more intense rainfall seasonality at the Iberian Peninsula, as suggested by pollen records (Oliveira et al., 2016; Desprat et al., 2004; Tzedakis et al., 2009) and the description of early MIS 11c as a humid period affecting the Mediterranean and the North Atlantic region (Helmke et al., 2008; Kandiano et al., 2012).

The prolonged mild conditions during winter and reduced wind field over the NW Mediterranean most likely resulted in a decreased WMDW formation. A low AJ influx has clearly been traced by the low N and percentages of *G. oceanica* (Fig. 6h). The decrease in abundance of *H. carteri* and *Syracosphaera* spp. (Fig. 5e and f) suggests less turbid and fresher surface layer conditions than during the MIS 12/MIS 11 transition. An extended surface warm water scenario, as indicated by the high SST (Fig. 6b), is somewhat at odds with the decrease in percentages and N of the WWT until 413 kyr in our coccolithophore record (Fig. 5c) and the parallel rise in δ^{18}O from TV (Fig. 6a). Reconciliations of these results may lie in the reduction inflow of surface AW into the Alboran Sea. Indeed, the decrease in δ^{13}C from *G. bulloides* at 413.5 kyr (Fig. 6e) could be interpreted as the expression of the transference of reduced intermediate water ventilation to surface. Sediment trap studies in the region reported a high affinity of this foraminifera species for upwelling conditions (Bárcena et al., 2004; Hernández-Alméida et al., 2011); thus, an imprint of the subsurface geochemical conditions in its isotopic profile is considered. This pattern was furthermore coeval with the deposition of sapropel S11 and the weak ventilation of intermediate and bottom waters in the eastern Mediterranean (Konijnendijk et al., 2014). A similar δ^{13}C response in the western Mediterranean was described at nearby Site 975 during the humid period of the early Holocene and the deposition of ORL 1 (Jimenez-Espejo et al., 2008). Furthermore, the coccolithophore primary productivity reconstruction by Colmenero-Hidalgo et al. (2004) during this early Holocene period also agrees with the lower PPP observed here during the early MIS 11c (Fig. 5c). The suggested limitation in the western Mediterranean circulation ultimately agrees with the weakening in the intensity of the MOW after Termination V, as reported by Sánchez-Goñi et al. (2016).

A shift to a more intense *Alboran Upwelling System* from 405 kyr across the late MIS 11c is suggested from an increase in the PPP and the percentages of small *Gephyrocapsa* (Fig. 6c and d). A relationship with an intra-interglacial northward shift of the temperate westerlies through a + NAO-*like* phase is evidenced by the increased phytolith content (Fig. 6f) and the long-term forest decline at Site U1385 (Fig. 6g). These results point to a latitudinal aridification and are in agreement with the terrestrial moisture decrease and cooling of SW Iberia (Oliveira et al., 2016) and the enhanced Saharan dust flux towards Site 958 from ~405 kyr (Helmke et al., 2008). More constant peaks of heavy planktonic δ^{13}C values (Fig. 6e) indicate intense surface nutrient supply coupled with high nutrient consumption rates, that further support the occurrence of an additional nutrient fertilization by the Saharan dust supply into the Alboran Sea. The high N and percentages of *G. oceanica* (Fig. 6h), together with the high abundances of *H. carteri* and *Syracosphaera* spp. (Fig. 4e and f), shows an intensified AJ and surface circulation. The moderate increase in the N of the reworked nannofossils is tentatively proposed to be linked to the depositional

processes related to intensified deep circulation in the Alboran Sea.

The increased percentages and N maxima of the WWT, from 410 kyr onwards (Fig. 5c), are interpreted to reflect an intensification of the AzC over the study region and are in agreement with previous studies (Marino et al., 2018). From a coccolithophore perspective, the intra-interglacial intensification of the *Alboran Upwelling System* shares many similarities with the timing of the development of the Alboran Gyres during the Holocene (Rohling et al., 1995; Pérez-Folgado et al., 2003), which were described by marked increases in coccolithophore productivity between 8.2 kyr (Colmenero-Hidalgo et al., 2004) and 7.7 kyr (Ausín et al., 2015b). This Holocene hydrological shift has been suggested to be related to cold and arid continental conditions (cold and arid Holocene 8.2 kyr event; Alley et al., 1997). The terrestrial climate during MIS 11c is characterized in several records by a vegetation setback during the "Older Holsteinian Oscillation" event (Koutsodendris et al., 2012). The comparable response of the *Alboran Upwelling System* supports the previously proposed relationship of the "Older Holsteinian Oscillation" event of the late MIS 11 (Koutsodendris et al., 2012) and the middle (8.2 kyr; Koutsodendris et al., 2012) to the late (Combourieu-Nebout et al., 2009; Desprat et al., 2013) Holocene arid event (see Oliveira et al., 2016 and references therein).

5.4. MIS 11 b and MIS 11a

During MIS 11 b and MIS 11a, an intense *Alboran Upwelling System* is identified from the high PPP and percentages of small *Gephyrocapsa* (Fig. 6c and d). There are two important exceptions that are coeval with the Heinrich-*type* events 3 and 2, that are discussed in section 5.5. A maintained + NAO-*like* atmospheric configuration phase after 397 kyr at the MIS 11c/MIS 11 b transition is suggested by the high phytolith content (Fig. 6f) and the long-term decline in Mediterranean forest pollen at Site U1385 (Fig. 6g). A shift towards year-round sustained humidity in SW Iberia (Oliveira et al., 2016) may have affected the phytolith transport activity and explain the decrease in records for 389-384 kyr and 382-376 kyr (Fig. 6f). The increased coccolith N and NAR (Fig. 3c and d), together with the lowered magnetic susceptibilities of the core sediments between 61.504–61.104 and 60.405–59.544 mbsf (Comas et al., 1996), reflect an enhancement in the biogenic carbonate sedimentation. This may explain a dilution of the phytolith concentrations in the sediments. The recovered increase in phytolith concentrations during MIS 11a (Fig. 6f) was consistent with the timing of increased aridification in N Africa, as described by Helmke et al. (2008) at ODP Site 958 towards the end of MIS 11.

While we lack direct evidences of MOW intensities during MIS 11 b and MIS 11a, the increased N and percentages of *G. oceanica* (Fig. 6h) are in agreement with the strengthening of the Mediterranean circulation and intensification of the AJ inflow, ultimately resulting in an intensification of the *Alboran Upwelling System*. We propose that cooler and more intense and prolonged evaporative conditions in the NW Mediterranean would have intensified the outflow of Mediterranean waters through the Strait of Gibraltar. Further evidence for the increased influence of the surface AW over the Alboran Sea is provided by the notable increase in the N values and percentages of *C. pelagicus* subsp. *azorinus* (Fig. 5g). This idea is supported by the findings of Parente et al. (2004), who proposed the use of this taxon as a proxy for the intensification of AH cells and the more vigorous influence of the Atlantic Azores Front over the Iberian margin.

5.5. Heinrich – type 3 and 2

Two pronounced drops in PPP centred at 390 and 383 kyr suggest an abrupt reduction in the activity of the *Alboran Upwelling System* (Fig. 6c and d). This shift was coeval with two rapid SST cooling events (Fig. 6b) and is accompanied by slight increases in the temperature-sensitive cold species *C. pelagicus* subsp. *pelagicus* (Fig. 5d) and *G. muellerae* (Fig. 4f), suggesting an influence of subpolar meltwaters in the western Mediterranean. The timing of these episodes is related to Heinrich-*type* (Ht) events 3 and 2 (Ht3 and Ht2), identified at the Portuguese Iberian margin Site MD03-2699, based on Rodrigues et al. (2011). These events have been linked to disruptions in the Atlantic Meridional Overturning Circulation, from iceberg discharge that originates from the British ice sheet (Rodrigues et al., 2011 and references therein).

The phytolith content was particularly increased during the Ht2 event (Fig. 6f), suggesting an enhancement in wind-driven transport from North Africa. Interestingly, the Ht3 and Ht2 events corresponded to the most severe and longest forest setbacks in SW Iberia (U1385-11-fe5 and fe6; Oliveira et al., 2016). The influences on both the terrestrial and marine ecosystems had significant similarities with the last glacial Heinrich stadial (HS; Cacho et al., 2000), suggesting a comparable atmospheric scenario of intensification and northward displacement of westerlies (Margari et al., 2010; Sánchez-Goñi et al., 2002; Oliveira et al., 2016). The moderate phytolith content of our record during this interval was thought to be due to the moderate degree of semi-desertic conditions in Iberia during the Ht3 and Ht2 events of MIS 11 in comparison with the HS of the last glacial period (Combourieu-Nebout et al., 2002; Sánchez Goñi et al., 2002).

According to our model, a persistent + NAO-*like* phase during these short stages is proposed. Analogous with that described during the HS events in the Mediterranean (Cacho et al., 2000), a consequent enhancement in the WMDW formation should occur. This hypothetical intensification in the western Mediterranean circulation during the Ht3 and Ht2 events is not clearly evidenced by a more intense *Alboran Upwelling System*, since our data suggests low PPP (Fig. 6c). However, high proportions of small *Gephyrocapsa*, reaching ~70% (Fig. 6d) provide evidence for an intense *Alboran Upwelling System*. We cannot discard the effects of temperature reductions on the production of *G. caribbeanica*, resulting in an overall decrease in PPP (Fig. 4d), as the species composing the small *Gephyrocapsa* group are better adapted to such abrupt temperature drops (Fig. 4c). The moderate increase in N and percentages of reworked nannofossils may indicate an intensification of deep circulations in the Alboran Sea during the Ht3 and Ht2 events (Fig. e).

6. Conclusions

Variations in the primary productivity proxy (PPP) and percentages of small *Gephyrocapsa* trace the changes in the coccolithophore paleoproductivity, triggered by the variations in the state of activation of the *Alboran Upwelling System* during the MIS 12/MIS 11 transition and MIS 11. A two-phase atmospheric scenario linked with the intensity of meridional atmospheric pressure gradients, NAO-*like*, is proposed to explain the changes in the state of activation of the *Alboran Upwelling System*:

1) Intensification in the activation of the *Alboran Upwelling System* corresponds with + NAO-*like* phase conditions, as evidenced by the enhanced phytolith content together with a decrease in the Mediterranean forest pollen records at IODP Site U1385. The more vigorous western Mediterranean circulation, induced by the enhanced WMDW formation in the NW Mediterranean during arid periods, is proposed to be a mechanism stimulating the complete gyre and offshore upwelling development from the intensified AJ influx. This scenario was identified during the

MIS 12/MIS 11 transition (428-422 kyr), the late MIS 11c (405-397 kyr), and MIS 11 b to MIS 11a (397-376).

2) Moderate activation of the *Alboran Upwelling System* corresponds with a - NAO-*like* phase, as suggested by a decrease in the phytolith content and maxima in the Mediterranean forest pollen record, at IODP Site U1385. The attenuated western Mediterranean circulation, due to a reduction of the WMDW formation during humid periods, is thought to hamper the complete upwelling development because there is a less intense AJ influx. This scenario is identified during the early MIS 11c (422-405 kyr).

During MIS 11 b, two short-term minima in PPP and SSTs, whose occurrences are centred 390 and 383 kyr, appear to be comparable with the Heinrich-*type* events Ht3 and Ht2 (Rodrigues et al., 2011 and references therein). Increased abundances of *C. pelagicus* subsp. *pelagicus* and *G. muellerae* is consistent with the inflow of cold surface waters into the Mediterranean Sea. A prolonged + NAO-*like* phase affecting the *Alboran Upwelling System* during these events is discussed.

Author statement

Coccolithophore sample analysis was made by AGL. Phytolith sample analysis was made by MAB. IC performed the isotopic analyses. JOG and AC processed and analysed the biomarkers for SST reconstruction. AGL integrated the data and conducted the research with the supervision of JAF. DO, ARH, MM, PM and LAA provided resources. AGL visualized and wrote the paper with the supervision of JAF and FJS and the input of coauthors. Founding acquisition leading to this publication was achieved by FJS and JAF.

Data statement

All data used in this study are available in the public repository PANGAEA® as: González-Lanchas, Alba; Flores, José-Abel; Sierro, Francisco J.; Bárcena, María Ángeles; Cortina, Aleix; Cacho, Isabel; Grimalt, Joan O (2020): Nannofossil, opal phytolith, stable isotopes and $U^{k'}_{37}$ Sea Surface Temperature record from ODP Site 977 during the MIS 11 https://doi.org/10.1594/PANGAEA.921235.

Declaration of competing interest

The authors declare that they have no known competing financial interests or personal relationships that could have appeared to influence the work reported in this paper.

Acknowledgments

This work was supported by the FPU contract of the Ministry of Education and Professional Formation of the Spanish government [FPU17/03349] awarded to A. González-Lanchas and by the financing infrastructure provided by the programs of the Ministry of Economy and Competitiveness [CGL 2015-68459-P] and the Ministry of Science, Innovation and Universities [RTI 2018-099489-B-100] granted to the GGO (Grupo de Geociencias Oceánicas) of the University of Salamanca. DO acknowledges funding from Portuguese Foundation for Science and Technology (FCT) through the CCMAR Research Unit - project UIDB/04326/2020 and contract (CEECIND/02208/2017). The authors thank Editor Antje Voelker and the two anonymous reviewers for their valuable comments and suggestions.

References

Alley, R.B., Mayewski, P.A., Sowers, T., Stuiver, M., Taylor, K.C., Clark, P.U., 1997. Holocene climatic instability: A prominent, widespread event 8200 yr ago. Geology 25 (6), 483–486.

Álvarez, M.C., Amore, F.O., Cros, L., Alonso, B., Alcántara-Carrió, J., 2010. Coccolithophore biogeography in the Mediterranean Iberian margin. Revista Española de Micropaleontología 42 (3), 359–371.

Amore, F.O., Flores, J.A., Voelker, A.H.L., Lebreiro, S.M., Palumbo, E., Sierro, F.J., 2012. A middle Pleistocene northeast atlantic coccolithophore record: paleoclimatology and paleoproductivity aspects. Mar. Micropaleontol. 90–91, 44–59.

Ausín, B., Flores, J.-A., Sierro, F.-J., Bárcena, M.-A., Hernández-Almeida, I., Francés, G., Gutiérrez-Arnillas, E., Martrat, B., Grimalt, J.O., Cacho, I., 2015a. Coccolithophore productivity and surface water dynamics in the Alboran Sea during the last 25 kyr. Palaeogeogr. Palaeoclimatol. Palaeoecol. 418, 126–140.

Ausín, B., Flores, J.A., Sierro, F.J., Cacho, I., Hernández-Almeida, I., Martrat, B., Grimalt, J.O., 2015b. Atmospheric patterns driving holocene productivity in the Alboran Sea (western mediterranean): a multiproxy approach. Holocene 25, 583–595.

Barber, R., Hiscock, M., 2006. A rising tide lifts all phytoplankton: growth response of other phytoplankton taxa in diatom-dominated blooms. Global Biogeochem. Cycles 20.

Bárcena, M.A., Abrantes, F., 1998. Evidence of a high-productivity area off the coast of Málaga from studies of diatoms in surface sediments. Mar. Micropaleontol. 35 (1–2), 91–103.

Bárcena, M., Cacho, I., Abrantes, F., Sierro, F., Grimalt, J., Flores, J., 2001. Paleoproductivity variations related to climatic conditions in the Alboran Sea (western Mediterranean) during the last glacial–interglacial transition: the diatom record. Palaeogeogr. Palaeoclimatol. Palaeoecol. 167, 337–357.

Bárcena, M., Flores, J., Sierro, F., Pérez-Folgado, M., Fabres, J., Calafat, A., Canals, M., 2004. Planktonic response to main oceanographic changes in the Alboran Sea (Western Mediterranean) as documented in sediment traps and surface sediments. Mar. Micropaleontol. 53, 423–445.

Barker, S., Archer, D., Booth, L., Elderfield, H., Henderiks, J., Rickaby, R.E., 2006. Globally increased pelagic carbonate production during the Mid-Brunhes dissolution interval and the CO2 paradox of MIS 11. Quat. Sci. Rev. 25, 3278–3293.

Barker, S., Chen, J., Gong, X., Jonkers, L., Knorr, G., Thornalley, D., 2015. Icebergs not the trigger for North Atlantic cold events. Nature 520, 333.

Bauch, H.A., Kandiano, E.S., Helmke, J.P., 2012. Contrasting ocean changes between the subpolar and polar North Atlantic during the past 135 ka. Geophys. Res. Lett. 39.

Baumann, K.-H., Andruleit, H., Böckel, B., Geisen, M., Kinkel, H., 2005. The significance of extant coccolithophores as indicators of ocean water masses, surface water temperature, and palaeoproductivity: a review. Paläontol. Z. 79, 93–112.

Baumann, K.-H., Böckel, B., Frenz, M., 2004. Coccolith Contribution to South Atlantic Carbonate Sedimentation, Coccolithophores. Springer, pp. 367–402.

Bazzicalupo, P., Maiorano, P., Girone, A., Marino, M., Combourieu-Nebout and, N., Incarbona, A., 2018. High-frequency climate fluctuations over the last deglaciation in the Alboran Sea, Western Mediterranean: evidence from calcareous plankton assemblages. Palaeogeogr. Palaeoclimatol. Palaeoecol. 506, 226–241.

Bazzicalupo, P., Maiorano, P., Girone, A., Marino, M., Combourieu-Nebout, N., Pelosi, N., Salgueiro, E., Incarbona, A., 2020. Holocene climate variability of the Western Mediterranean: surface water dynamics inferred from calcareous plankton assemblages. Holocene, 0959683619895580.

Berger, A., Loutre, M.F., 1991. Insolation values for the climate of the last 10 million years. Quat. Sci. Rev. 10 (4), 297–317.

Berger, W., Wefer, G., 2003. On the dynamics of the ice ages: stage-11 paradox, mid-Brunhes climate shift, and 100-ky cycle. GEOPHYSICAL MONOGRAPH-AMERICAN GEOPHYSICAL UNION 137, 41–60.

Boeckel, B., Baumann, K.-H., 2004. Distribution of coccoliths in surface sediments of the south-eastern South Atlantic Ocean: ecology, preservation and carbonate contribution. Mar. Micropaleontol. 51, 301–320.

Bollmann, J., Baumann, K.H., Thierstein, H.R., 1998. Global dominance of Gephyrocapsa coccoliths in the late Pleistocene: selective dissolution, evolution, or global environmental change? Paleoceanography 13, 517–529.

Brassell, S.C., Eglinton, G., Marlowe, I.T., Pflaumann, U., Sarnthein, M., 1986. Molecular stratigraphy: a new tool for climatic assessment. Nature 320 (6058), 129–133.

Cacho, I., Grimalt, J.O., Pelejero, C., Canals, M., Sierro, F.J., Flores, J.A., Shackleton, N., 1999. Dansgaard-oeschger and Heinrich event imprints in Alboran Sea paleotemperatures. Paleoceanography 14, 698–705.

Cacho, I., Grimalt, J.O., Sierro, F.J., Shackleton, N., Canals, M., 2000. Evidence for enhanced Mediterranean thermohaline circulation during rapid climatic coolings. Earth Planet Sci. Lett. 183, 417–429.

Candy, I., Schreve, D.C., Sherriff, J., Tye, G.J., 2014. Marine Isotope Stage 11: palaeoclimates, palaeoenvironments and its role as an analogue for the current interglacial. Earth Sci. Rev. 128, 18–51.

Carter, J.A., Lian, O.B., 2000. Palaeoenvironmental reconstruction from the last interglacial using phytolith analysis, southeastern North Island, New Zealand. J. Quat. Sci.: Published for the Quaternary Research Association 15, 733–743.

Combourieu-Nebout, N., Turon, J.-L., Zahn, R., Capotondi, L., Londeix, L., Pahnke, K., 2002. Enhanced aridity and atmospheric high-pressure stability over the western Mediterranean during the North Atlantic cold events of the past 50 ky.

Geology 30, 863–866.
Combourieu-Nebout, N., Peyron, O., Dormoy, I., Desprat, S., Beaudouin, C., Kotthoff, U., Marret, F., 2009. Rapid climatic variability in the west Mediterranean during the last 25 000 years from high resolution pollen data. Climate Past 5, 503–521.
Colmenero-Hidalgo, E., Flores, J.-A., Sierro, F.J., Bárcena, M.A., Löwemark, L., Schönfeld, J., Grimalt, J.O., 2004. Ocean surface water response to short-term climate changes revealed by coccolithophores from the Gulf of Cadiz (NE Atlantic) and Alboran Sea (W Mediterranean). Palaeogeogr. Palaeoclimatol. Palaeoecol. 205, 317–336.
Comas, M., Zahn, R., Klaus, A., 1996. Preliminary results of ODP leg 161. Proceeding Ocean Drilling Program, Preliminary Results 161, 1–1679.
Coplen, T.B., 1996. New guidelines for reporting stable hydrogen, carbon, and oxygen isotope-ratio data. Geochem. Cosmochim. Acta 60 (17), 3359–3360.
d'Ortenzio, F., Ribera d'Alcalà, M., 2009. On the trophic regimes of the Mediterranean Sea: a satellite analysis. Biogeosciences 6, 139–148.
Dai, A., Fung, I.Y., Del Genio, A.D., 1997. Surface observed global land precipitation variations during 1900–88. J. Clim. 10, 2943–2962.
de Abreu, L., Abrantes, F.F., Shackleton, N.J., Tzedakis, P.C., McManus, J.F., Oppo, D.W., Hall, M.A., 2005. Ocean climate variability in the eastern North Atlantic during interglacial marine isotope stage 11: a partial analogue to the Holocene? Paleoceanography 20, 1–15.
Desprat, S., Goñi, M.S., Naughton, F., Turon, J.-L., Duprat, J., Malaizé, B., Cortijo, E., Peypouquet, J.-P., 2007. Climate variability of the last five isotopic interglacials: direct land-sea-ice correlation from the multiproxy analysis of North-Western Iberian margin deep-sea cores. In: Developments in Quaternary Sciences. Elsevier, pp. 375–386.
Desprat, S., Sánchez Goñi, M.F., Naughton, F., Turon, J.-L., Duprat, J., Malaizé, B., Peypouquet, J.-P., Pujol, C., 2004. Climatic variability of the last five isotopic interglacials: direct land-sea correlation from multiproxy analyses of north-western Iberian margin deep-sea cores. In: 8th International Conference on Paleoceanography: ICP-8.
Desprat, S., Combourieu-Nebout, N., Essallami, L., Sicre, M.A., Dormoy, I., Peyron, O., Siani, G., Bout Roumazeilles, V., Turon, J.L., 2013. Deglacial and Holocene vegetation and climatic changes in the southern central Mediterranean from a direct land-sea correlation. Climate Past 9, 767–787.
Droxler, A.W., Farrell, J.W., 2000. Marine Isotope Stage 11 (MIS 11): new insights for a warm future. Global Planet. Change 24, 1–5.
Fenoglio-Marc, L., Mariotti, A., Sannino, G., Meyssignac, B., Carillo, A., Struglia, M.V., Rixen, M., 2013. Decadal variability of net water flux at the Mediterranean Sea Gibraltar Strait. Global Planet. Change 100, 1–10.
Fletcher, W.J., Debret, M., Sánchez-Goñi, M.F., 2013. Mid-Holocene emergence of a low-frequency millennial oscillation in western Mediterranean climate: implications for past dynamics of the North Atlantic atmospheric westerlies. Holocene 23, 153–166.
Flores, J., Sierro, F., 1997. Revised technique for calculation of calcareous nannofossil accumulation rates. Micropaleontology 321–324.
Flores, J.A., Bárcena, M.A., Sierro, F.J., 2000. Ocean-surface and wind dynamics in the atlantic ocean off northwest Africa during the last 140 000 years. Palaeogeogr. Palaeoclimatol. Palaeoecol. 161 (3–4), 459–478.
Flores, J.A., Filippelli, G.M., Sierro, F.J., Latimer, J.C., 2012. The "White Ocean" hypothesis: a late Pleistocene Southern Ocean governed by coccolithophores and driven by phosphorus. Front. Microbiol. 3, 233.
Flores, J.A., Marino, M., 2002. Pleistocene calcareous nannofossil stratigraphy for ODP leg 177 (atlantic sector of the southern ocean). Mar. Micropaleontol. 45, 191–224.
Frigola, J., Moreno, A., Cacho, I., Canals, M., Sierro, F.J., Flores, J.A., Grimalt, J.O., Hodell, D.A., Curtis, J.H., 2007. Holocene climate variability in the western Mediterranean region from a deepwater sediment record. Paleoceanography 22.
Garcia-Gorriz, E., Carr, M.E., 1999. The climatological annual cycle of satellite-derived phytoplankton pigments in the Alboran Sea. Geophys. Res. Lett. 26, 2985–2988.
Gartner, S., 1988. Paleoceanography of the mid-Pleistocene. Mar. Micropaleontol. 13, 23–46.
Geisen, M., Billard, C., Broerse, A.T., Cros, L., Probert, I., Young, J.R., 2002. Life-cycle associations involving pairs of holococcolithophorid species: intraspecific variation or cryptic speciation? Eur. J. Phycol. 37, 531–550.
Giraudeau, J., 1992. Distribution of recent nannofossils beneath the Benguela system: southwest African continental margin. Mar. Geol. 108, 219–237.
Girone, A., Maiorano, P., Marino, M., Kucera, M., 2013. Calcareous plankton response to orbital and millennial-scale climate changes across the Middle Pleistocene in the western Mediterranean. Palaeogeogr. Palaeoclimatol. Palaeoecol. 392, 105–116.
Heburn, G.W., La Violette, P.E., 1990. Variations in the structure of the anticyclonic gyres found in the Alboran Sea. J. Geophys. Res.: Oceans 95, 1599–1613.
Helmke, J.P., Bauch, H.A., Röhl, U., Kandiano, E.S., 2008. Uniform climate development between the subtropical and subpolar Northeast Atlantic across marine isotope stage 11. Clim. Past Discuss 4, 433–457.
Hernández-Almeida, I., Bárcena, M., Flores, J., Sierro, F., Sanchez-Vidal, A., Calafat, A., 2011. Microplankton response to environmental conditions in the Alboran Sea (Western Mediterranean): one year sediment trap record. Mar. Micropaleontol. 78, 14–24.
Hodell, D.A., Charles, C.D., Ninnemann, U.S., 2000. Comparison of interglacial stages in the South Atlantic sector of the southern ocean for the past 450 kyr: implications for Marine Isotope Stage (MIS) 11. Global Planet. Change 24, 7–26.
Hodell, D., Crowhurst, S., Skinner, L., Tzedakis, P.C., Margari, V., Channell, J.E., Kamenov, G., Maclachlan, S., Rothwell, G., 2013. Response of Iberian Margin sediments to orbital and suborbital forcing over the past 420 ka. Paleoceanography 28, 185–199.
Hurrell, J.W., 1995. Decadal trends in the North Atlantic Oscillation: regional temperatures and precipitation. Science 269, 676–679.
Incarbona, A., Di Stefano, E., Bonomo, S., 2009. Calcareous nannofossil biostratigraphy of the central Mediterranean Basin during the last 430 000 years. Stratigraphy 6 (1), 33–34.
Jansen, J., Kuijpers, A., Troelstra, S., 1986. A mid-Brunhes climatic event: long-term changes in global atmosphere and ocean circulation. Science 232, 619–622.
Jimenez-Espejo, F., Martinez-Ruiz, F., Rogerson, M., González-Donoso, J., Romero, O., Linares, D., Sakamoto, T., Gallego-Torres, D., Rueda Ruiz, J., Ortega-Huertas, M., 2008. Detrital input, productivity fluctuations, and water mass circulation in the westernmost Mediterranean Sea since the Last Glacial Maximum. G-cubed 9.
Johnson, J., Stevens, I., 2000. A fine resolution model of the eastern North Atlantic between the Azores, the canary islands and the Gibraltar strait. Deep Sea Res. Oceanogr. Res. Pap. 47 (5), 875–899.
Kandiano, E.S., Bauch, H.A., Fahl, K., Helmke, J.P., Röhl, U., Pérez-Folgado, M., Cacho, I., 2012. The meridional temperature gradient in the eastern North Atlantic during MIS 11 and its link to the ocean–atmosphere system. Palaeogeogr. Palaeoclimatol. Palaeoecol. 333, 24–39.
Knappertsbusch, M., 1993. Geographic distribution of living and holocene coccolithophores in the Mediterranean Sea. Mar. Micropaleontol. 21, 219–247.
Konijnendijk, T.Y.M., Ziegler, M., Lourens, L.J., 2014. Chronological constraints on Pleistocene sapropel depositions from high-resolution geochemical records of ODP sites 967 and 968. Newsl. Stratigr. 47, 263–282.
Koutsodendris, A., Müller, U.C., Pross, J., Brauer, A., Kotthoff, U., Lotter, A.F., 2010. Vegetation dynamics and climate variability during the Holsteinian interglacial based on a pollen record from Dethlingen (northern Germany). Quat. Sci. Rev. 29, 3298–3307.
Koutsodendris, A., Pross, J., Müller, U.C., Brauer, A., Fletcher, W.J., Kühl, N., Kirilova, E., Verhagen, F.T.M., Lücke, A., Lotter, A.F., 2012. A short-term climate oscillation during the Holsteinian interglacial (MIS 11c): an analogy to the 8.2ka climatic event? Glob. Planet. Change 92-93, 224–235.
Lafuente, J.G., Vargas, J.M., Plaza, F., Sarhan, T., Candela, J., Bascheck, B., 2000. Tide at the eastern section of the Strait of Gibraltar. J. Geophys. Res.: Oceans 105, 14197–14213.
Lionello, P., 2012. The Climate of the Mediterranean Region: from the Past to the Future. Elsevier.
Lisiecki, L.E., Raymo, M.E., 2005. A Pliocene-Pleistocene stack of 57 globally distributed benthic δ18O records. Paleoceanography 20.
Loutre, M.-F., Berger, A., 2003. Marine Isotope Stage 11 as an analogue for the present interglacial. Global Planet. Change 36, 209–217.
Maiorano, P., Marino, M., Balestra, B., Flores, J.A., Hodell, D.A., Rodrigues, T., 2015. Coccolithophore variability from the shackleton site (IODP site U1385) through MIS 16-10. Global Planet. Change 133, 35–48.
Margari, V., Skinner, L., Tzedakis, P., Ganopolski, A., Vautravers, M., Shackleton, N., 2010. The nature of millennial-scale climate variability during the past two glacial periods. Nat. Geosci. 3, 127.
Marino, M., Girone, A., Maiorano, P., Di Renzo, R., Piscitelli, A., Flores, J.A., 2018. Calcareous plankton and the mid-Brunhes climate variability in the Alboran Sea (ODP Site 977). Palaeogeogr. Palaeoclimatol. Palaeoecol. 508, 91–106.
Marino, M., Maiorano, P., Tarantino, F., Voelker, A., Capotondi, L., Girone, A., Lirer, F., Flores, J.A., Naafs, B.D.A., 2014. Coccolithophores as proxy of seawater changes at orbital-to-millennial scale during middle Pleistocene Marine Isotope Stages 14–9 in North Atlantic core MD01-2446. Paleoceanography 29, 518–532.
Martrat, B., Grimalt, J.O., Lopez-Martinez, C., Cacho, I., Sierro, F.J., Flores, J.A., Zahn, R., Canals, M., Curtis, J.H., Hodell, D.A., 2004. Abrupt temperature changes in the Western Mediterranean over the past 250,000 years. Science 306, 1762–1765.
Martrat, B., Grimalt, J.O., Shackleton, N.J., de Abreu, L., Hutterli, M.A., Stocker, T.F., 2007. Four climate cycles of recurring deep and surface water destabilizations on the iberian margin. Science 317, 502–507.
McManus, J., Oppo, D., Cullen, J., Healey, S., 2003. Marine isotope stage 11 (MIS 11): analog for holocene and future climate? Geophys. Monogr. 69–85.
Millot, C., 1999. Circulation in the western Mediterranean Sea. J. Mar. Syst. 20, 423–442.
Millot, C., 2008. Short-term variability of the Mediterranean in-and out-flows. Geophys. Res. Lett. 35 (15).
Moreno, A., Cacho, I., Canals, M., Prins, M.A., Sánchez-Goñi, M.-F., Grimalt, J.O., Weltje, G.J., 2002. Saharan dust transport and high-latitude glacial climatic variability: the Alboran Sea record. Quat. Res. 58, 318–328.
Moulin, C., Lambert, C.E., Dulac, F., Dayan, U., 1997. Control of atmospheric export of dust from North Africa by the north atlantic oscillation. Nature 387, 691.
Müller, P.J., Kirst, G., Ruhland, G., Von Storch, I., Rosell-Melé, A., 1998. Calibration of the alkenone paleotemperature index U37K′ based on core-tops from the eastern South Atlantic and the global ocean (60° N-60° S). Geochimica et Cosmochimica Acta 62 (10), 1757–1772.
Oliveira, D., Desprat, S., Rodrigues, T., Naughton, F., Hodell, D., Trigo, R., Rufino, M., Lopes, C., Abrantes, F., Sánchez-Goñi, M.F., 2016. The complexity of millennial-scale variability in southwestern Europe during MIS 11. Quat. Res. 86, 373–387.

Olson, S.L., Hearty, P.J., 2009. A sustained +21m sea-level highstand during MIS 11 (400ka): direct fossil and sedimentary evidence from Bermuda. Quat. Sci. Rev. 28, 271–285.
Oppo, D., McManus, J., Cullen, J., 1998. Abrupt climate events 500,000 to 340,000 years ago: evidence from subpolar North Atlantic sediments. Science 279, 1335–1338.
Packard, T.T., Minas, H., Coste, B., Martinez, R., Bonin, M., Gostan, J., Garfield, P., Christensen, J., Dortch, Q., Minas, M., 1988. formation of the alboran oxygen minimum zone. Deep sea research Part A. Oceanographic Research Papers 35, 1111–1118.
Past Interglacials Working Group of PAGES, 2016. Interglacials of the last 800,000 years. Rev. Geophys. 54 (1), 162–219.
Palumbo, E., Flores, J.A., Perugia, C., Emanuele, D., Petrillo, Z., Rodrigues, T., Voelker, A.H., Amore, F.O., 2013. Abrupt variability of the last 24 ka BP recorded by coccolithophore assemblages off the Iberian Margin (core MD03-2699). J. Quat. Sci. 28, 320–328.
Parente, A., Cachão, M., Baumann, K.-H., de Abreu, L., Ferreira, J., 2004. Morphometry of Coccolithus pelagicus sl (Coccolithophore, Haptophyta) from offshore Portugal, during the last 200 kyr. Micropaleontology 50, 107–120.
Parrilla, G., Kinder, T.H., 1987. Oceanografía física del mar de Alborán, vol. 4. Boletín del Instituto Español de Oceanografía, pp. 133–165.
Perkins, H., Kinder, T., Violette, P.L., 1990. The atlantic inflow in the western Alboran Sea. J. Phys. Oceanogr. 20, 242–263.
Pérez-Folgado, M., Sierro, F.J., Flores, J.A., Cacho, I., Grimalt, J.O., Zahn, R., Shackleton, N., 2003. WesternMediterranean planktonic foraminifera events and millennial climatic variability during the last 70 kyr. Mar. Micropaleontol. 48, 49–70.
Pistek, P., De Strobel, F., Montanari, C., 1985. Deep-sea circulation in the Alboran Sea. J. Geophys. Res.: Oceans 90, 4969–4976.
Prahl, F.G., Wakeham, S.G., 1987. Calibration of unsaturation patterns in long-chain ketone compositions for palaeotemperature assessment. Nature 330 (6146), 367–369.
Prokopenko, A., Bezrukova, E., Khursevich, G., Solotchina, E., Kuzmin, M., Tarasov, P., 2010. Climate in continental interior Asia during the longest interglacial of the past 500 000 years: the new MIS 11 records from Lake Baikal, SE Siberia. Clim. Past 6, 31–48.
Quézel, P., Médail, F., 2003. Que faut-il entendre par" forêts méditerranéennes. Forêt méditerranéenne 24, 11–31.
Railsback, L.B., Gibbard, P.L., Head, M.J., Voarintsoa, N.R.G., Toucanne, S., 2015. An optimized scheme of lettered marine isotope substages for the last 1.0 million years, and the climatostratigraphic nature of isotope stages and substages. Quat. Sci. Rev. 111, 94–106.
Raymo, M.E., Mitrovica, J.X., 2012. Collapse of polar ice sheets during the stage 11 interglacial. Nature 483, 453.
Raynaud, D., Barnola, J.-M., Souchez, R., Lorrain, R., Petit, J.-R., Duval, P., Lipenkov, V.Y., 2005. Palaeoclimatology: the record for marine isotopic stage 11. Nature 436, 39.
Reyes, A.V., Carlson, A.E., Beard, B.L., Hatfield, R.G., Stoner, J.S., Winsor, K., Welke, B., Ullman, D.J., 2014. South Greenland ice-sheet collapse during marine isotope stage 11. Nature 510, 525.
Rigual-Hernández, A.S., Bárcena, M.A., Jordan, R.W., Sierro, F.J., Flores, J.A., Meier, K.S., Heussner, S., 2013. Diatom fluxes in the NW Mediterranean: evidence from a 12-year sediment trap record and surficial sediments. J. Plankton Res. 35 (5), 1109–1125.
Roberts, D.L., Karkanas, P., Jacobs, Z., Marean, C.W., Roberts, R.G., 2012. Melting ice sheets 400,000 yr ago raised sea level by 13 m: Past analogue for future trends. Earth Planet Sci. Lett. 357, 226–237.
Rodó, X., Baert, E., Comin, F., 1997. Variations in seasonal rainfall in southern europe during the present century: relationships with the north atlantic oscillation and the el niño-southern oscillation. Clim. Dynam. 13, 275–284.
Rodrigues, T., Voelker, A., Grimalt, J., Abrantes, F., Naughton, F., 2011. Iberian Margin sea surface temperature during MIS 15 to 9 (580–300 ka): glacial suborbital variability versus interglacial stability. Paleoceanography 26.
Rogerson, M., Rohling, E., Bigg, G.R., Ramirez, J., 2012. Paleoceanography of the Atlantic-Mediterranean exchange: overview and first quantitative assessment of climatic forcing. Rev. Geophys. 50.
Rohling, E.J., Den Dulk, M., Pujol, C., Vergnaud-Grazzini, C., 1995. Abrupt hydrographic change in the Alboran Sea (western Mediterranean) around 8000 yrs BP. Deep-Sea Res. I Oceanogr. Res. Pap. 42, 1609–1619.
Rohling, E.J., Fenton, M., Jorissen, F.J., Bertrand, P., Ganssen, G., Caulet, J.P., 1998. Magnitudes of sea-level lowstands of the past 500,000 years. Nature 394, 162–165.
Rohling, E.J., Braun, K., Grant, K., Kucera, M., Roberts, A.P., Siddall, M., Trommer, G., 2010. Comparison between holocene and marine isotope stage-11 sea-level histories. Earth Planet Sci. Lett. 291, 97–105.
Saavedra-Pellitero, M., Baumann, K.H., Lamy, F., Köhler, P., 2017. Coccolithophore variability across marine isotope stage 11 in the pacific sector of the southern ocean and its potential impact on the carbon cycle. Paleoceanography 32, 864–880.
Salat, J., Cruzado, A., 1981. Masses d'eau dans la Mediterranee Occidentale: mer Catalane et eaux adjacentes. Rapp. Comm. Int. Exploit. Sci. Mer Mediterranee 27, 201–209.
Sánchez-Goñi, M.F., Cacho, I., Turon, J.-L., Guiot, J., Sierro, F., Peypouquet, J., Grimalt, J., Shackleton, N., 2002. Synchroneity between marine and terrestrial responses to millennial scale climatic variability during the last glacial period in the Mediterranean region. Clim. Dynam. 19, 95–105.
Sánchez-Goñi, M.F., Llave, E., Oliveira, D., Naughton, F., Desprat, S., Ducassou, E., et al., 2016. Climate changes in south western Iberia and Mediterranean Outflow variations during two contrasting cycles of the last 1 Myrs: MIS 31–MIS 30 and MIS 12–MIS 11. Global Planet. Change 136, 18–29.
Sanchez-Vidal, A., Calafat, A., Canals, M., Frigola, J., Fabres, J., 2005. Particle fluxes and organic carbon balance across the eastern Alboran Sea (SW Mediterranean Sea). Continent. Shelf Res. 25, 609–628.
Sarhan, T., Lafuente, J.G., Vargas, M., Vargas, J.M., Plaza, F., 2000. Upwelling mechanisms in the northwestern Alboran Sea. J. Mar. Syst. 23, 317–331.
Sarnthein, M., Thiede, J., Pflaumann, U., Erlenkeuser, H., Fütterer, D., Koopmann, B., Lange, H., Seibold, E., 1982. Atmospheric and Oceanic Circulation Patterns off Northwest Africa during the Past 25 Million Years, Geology of the Northwest African Continental Margin. Springer, pp. 545–604.
Sierro, F.J., Hodell, D.A., Curtis, J.H., Flores, J.A., Reguera, I., Colmenero-Hidalgo, E., Bárcena, M.A., Grimalt, J.O., Cacho, I., Frigola, J., Canals, M., 2005. Impact of iceberg melting on Mediterranean thermohaline circulation during Heinrich events. Paleoceanography 20, 1–13.
Siokou-Frangou, I., Christaki, U., Mazzocchi, M., Montresor, M., d'Alcalá, M.R., Vaqué, D., Zingone, A., 2009. Plankton in the open Mediterranean Sea: a review. Biogeosci. Discuss. 6.
Stein, R., Hefter, J., Grützner, J., Voelker, A., Naafs, B.D.A., 2009. Variability of surface water characteristics and heinrich-like events in the Pleistocene midlatitude North Atlantic ocean: biomarker and XRD records from IODP site U1313 (MIS 16–9). Paleoceanography 24.
Steinmetz, J.C., 1994. Sedimentation of coccolithophores. In: Coccolithophores. Cambridge University Press, Cambridge, pp. 179–197.
Stolz, K., Baumann, K.H., 2010. Changes in palaeoceanography and palaeoecology during Marine Isotope Stage (MIS) 5 in the eastern North Atlantic (ODP Site 980) deduced from calcareous nannoplankton observations. Palaeogeogr. Palaeoclimatol. Palaeoecol. 292 (1-2), 295–305.
Sumner, G., Homar, V., Ramis, C., 2001. Precipitation seasonality in eastern and southern coastal Spain. Int. J. Climatol. 21, 219–247.
Takahashi, K., Okada, H., 2000. Environmental control on the biogeography of modern coccolithophores in the southeastern Indian Ocean offshore of Western Australia. Mar. Micropaleontol. 39, 73–86.
Trigo, R.M., Osborn, T.J., Corte-Real, J.M., 2002. The North Atlantic Oscillation influence on Europe: climate impacts and associated physical mechanisms. Clim. Res. 20, 9–17.
Twiss, P.C., 1992. Predicted World Distribution of C 3 and C 4 Grass Phytoliths, Phytolith Systematics. Springer, pp. 113–128.
Tye, G., Sherriff, J., Candy, I., Coxon, P., Palmer, A., McClymont, E., Schreve, D., 2016. The δ18O stratigraphy of the Hoxnian lacustrine sequence at Marks Tey, Essex, UK: implications for the climatic structure of MIS 11 in Britain. J. Quat. Sci. 31, 75–92.
Tzedakis, P.C., Pälike, H., Roucoux, K.H., de Abreu, L., 2009. Atmospheric methane, southern European vegetation and low-mid latitude links on orbital and millennial timescales. Earth Planet Sci. Lett. 277, 307–317.
Villanueva, J., Pelejero, C., Grimalt, J.O., 1997. Clean-up procedures for the unbiased estimation of C37 alkenone sea surface temperatures and terrigenous n-alkane inputs in paleoceanography. J. Chromatogr. A 757 (1–2), 145–151.
Voelker, A.H., Rodrigues, T., Billups, K., Oppo, D.W., McManus, J.F., Stein, R., Hefter, J., Grimalt, J.O., 2010. Variations in mid-latitude North Atlantic surface water properties during the mid-Brunhes (MIS 9–14) and their implications for the thermohaline circulation. Clim. Past 6, 531–552.
Weaver, P., Pujol, C., 1988. History of the last deglaciation in the Alboran Sea (western mediterranean) and adjacent North Atlantic as revealed by coccolith floras. Palaeogeogr. Palaeoclimatol. Palaeoecol. 64, 35–42.
Winter, A., 1994. Biogeography of Living Coccolithophores in Ocean Waters. Coccolithophores.
Yin, Q.Z., Berger, A., 2012. Individual contribution of insolation and CO2 to the interglacial climates of the past 800,000 years. Clim. Dynam. 38, 709–724.
Young, J., Geisen, M., Cros, L., Kleijne, A., Sprengel, C., Probert, I., Østergaard, J., 2003. A guide to extant coccolithophore taxonomy. Journal of Nannoplankton Research, Special Issue 1, 1–132.
Young, J.R., Thierstein, H.R., Winter, A., 2000. Nannoplankton ecology and palaeoecology. Mar. Micropaleontol. 39, vii–ix.